LA-10543-MS

UC-70
Issued: October 1985

LA--10543-MS

DE86 007579

Mineralogic Summary of Yucca Mountain, Nevada

D. L. Bish
D. T. Vaniman

Los Alamos
Los Alamos National Laboratory
Los Alamos, New Mexico 87545

MINERALOGIC SUMMARY OF YUCCA MOUNTAIN, NEVADA

by

D. L. Bish and D. T. Vaniman

ABSTRACT

Quantitative x-ray powder diffraction analysis of tuffs and silicic lavas, using matrix-flushing techniques, has been used to obtain a model of three-dimensional mineral distributions at Yucca Mountain, Nevada. This method of analysis is especially useful in tuff, where the most abundant phases are commonly too fine grained for optical determination. The three-dimensional distributions of primary glass and of tridymite are particularly well constrained. Vitric nonwelded glasses occur above and below the welded devitrified Topopah Spring Member, but the glass in the lower nonwelded vitric zone is progressively altered to zeolites to the east where the zone is closer to the static water level. The zeolites clinoptilolite, mordenite, heulandite, and erionite have all been found at Yucca Mountain, but only mordenite and clinoptilolite are abundant and can be mapped between many drill holes and at many depths. Heulandite distribution is also mappable, but only below the densely welded devitrified part of the Topopah Spring Member. Erionite has been confirmed only once, as a fracture coating. There is a fairly continuous smectite-rich interval immediately above the basal vitrophyre of the Topopah Spring Member, but no evidence suggests that the smectites can provide information on the paleogroundwater table. There are at least four mappable zeolitized zones in Yucca Mountain, and the thicker zones tend to coincide with intervals that retained glass following early tuff devitrification. Problems in extrapolation occur where zones of welding pinch out. No phillipsite has been found, and some samples previously reported to contain phillipsite or erionite were reexamined with negative results. The deeper alteration to albite and analcime was not sampled in every drill hole, and the distribution of these phases is difficult to map.

I. INTRODUCTION

Yucca Mountain and surroundings, near the southwestern boundary of the Nevada Test Site (NTS) in south-central Nevada, are being studied to assess the suitability of the area to host a geologic repository for high-level radioactive waste. Research in this area, sponsored by the Nevada Nuclear Waste Storage Investigations (NNWSI) project of the U.S. Department of Energy (DOE), includes detailed studies of the mineralogy and petrology of the rocks in and surrounding Yucca Mountain. Results of these studies (Bish et al. 1981; Caporuscio et al. 1982; Levy 1984a; Vaniman et al. 1984) are yielding a detailed three-dimensional model of the Yucca Mountain area and are particularly important in predicting the effects a repository would have on the ground-water/rock system (Bish et al. 1984a). An integral part of mineralogy-petrology studies is the analysis of the rocks to determine the phases present. This has been done by x-ray powder diffraction (XRD) on the rocks at Yucca Mountain, which often have a very fine-grained groundmass that is not amenable to quantitative mineral analysis by optical techniques (Byers, 1985). Because rocks in Yucca Mountain will provide the ultimate containment of radioactive wastes, it is important that we have a thorough knowledge of the distribution of potentially sorptive and changeable phases. To understand the relationship between retardation of radionuclides and the phases present in the repository environment, studies are underway to test the correlation between mineralogy and sorption for numerous radionuclides (Bish et al. 1984b). These investigations have shown that the minerals clinoptilolite, mordenite, and smectite have particularly high sorption ratios for many cationic radionuclides.

Smyth (1982) and Bish et al. (1981) have discussed the potential for reaction of clinoptilolite and smectite to other minerals (e.g., analcime and lite) in a repository environment in the rocks at Yucca Mountain. These reactions occur primarily in response to increased temperatures and can produce significant amounts of water and result in volume decreases. Therefore, it is necessary to know the mineral distribution near the proposed repository horizon to avoid or plan for such potential reactions in construction. Lappin (1982) and Lappin et al. (1982) related the thermal properties of tuff, including matrix thermal conductivity and thermal expansion, to the bulk-rock mineralogy. They also discussed the relationship between mechanical properties and mineralogy, pointing out that additional data on rock fabric are required to predict bulk properties accurately. X-ray data on Yucca Mountain tuff samples also explain some variations in mechanical properties of the tuffs (Price et al. 1984).

This preliminary report summarizes current investigations of Yucca Mountain mineralogy. In addition, this report describes the methods used to obtain the data and the limitations of the data. Finally, it addresses questions about the occurrence of erionite and the relationship of mineralogy to paleogroundwater table.

II. ANALYTICAL TECHNIQUES

Sample Handling, Analysis, and Identification

The x-ray data presented in the appendix were obtained either on core and sidewall samples, for which accurate depth designations are given, or on drill cuttings samples, for which depths are approximate within a range of about 10 ft (3.28 m). Where core was available, 15 to 20 g of material were crushed in a shatterbox to provide a large, homogeneous sample. A portion of this powder was ground in a mortar and pestle under acetone to approximately -325 mesh (45 µm). A modification of this procedure was applied to the most recent analysis of samples from USW WT-1 and USW WT-2, which were ground under acetone in an automatic Brinkmann Retsch mill with agate mortar and pestle to less than 5 µm. This fine crystallite size is necessary to ensure adequate particle statistics (Klug and Alexander, 1974, pp. 365-367).

The resultant fine powder was gently packed into a 22- X 44-mm cavity in a glass slide; this cavity area is sufficient for the sample area to fully contain the x-ray beam at the lowest angle of interest. All unused powdered samples were stored in plastic vials. Samples from Drill Hole USW G-4 were mounted on a sample spinner in the diffractometer; the other samples were examined stationary.

All diffraction patterns were obtained on a Siemens D-500 powder diffractometer using a copper-target x-ray tube and a diffracted-beam monochromater. The diffractometer was run from 2.0° to 36.0° 2θ in the continuous scan mode at a scanning rate of 1°/min for samples from Drill Hole USW G-2 and G-4. Data for the remaining samples were collected automatically in the step scan mode with a step size of 0.02° 2θ and count times between 1.2 and 2.0 s per step. Several samples were run for count times up to 55 s per step to improve detection limits and to check for trace phases.

Minerals were identified by comparison of observed patterns to standard patterns produced in this laboratory and by comparison to published standards from the Joint Committee on Powder Diffraction Standards (JCPDS). Clay mineral standards were obtained from the Clay Minerals Society Source Clay Repository, and zeolite standards were recently obtained from Minerals Research Corporation, Clarkson, New York.

Quantitative Measurements

In contrast to qualitative identifications of the phases present in tuffs, quantitative multicomponent analysis is more difficult, time consuming, and is not straightforward because of a number of factors. These factors include variations in the degree of preferred orientation of crystallites, variations in crystallite size, variations in degree of crystallinity, and variations in composition (crystalline solid solution). In addition, the complex diffraction patterns often show peaks from at least six major phases, and the method of intensity measurement where there are complex peak overlaps affects quantitative results. Finally, because standards are required for quantitative analysis, the choice of standards plays a critical role. In our investigation, both natural materials and computer-calculated patterns were used as standards.

In order to eliminate or minimize the above sample problems, samples were finely ground as described above. Variations in feldspar composition were partially overcome by choosing x-ray diffraction lines that are not significantly affected by crystalline solid solution. Variations in the compositions of other minerals, e.g., clinoptilolite, mordenite, and smectite, were not compensated for, but errors thus introduced are likely to be smaller than those introduced by orientation effects and by problems with peak overlap. All of our analyses used integrated peak intensities (area measurements) rather than peak heights to compensate for variations in the degree of crystallinity.

Integrated intensities for all but USW G-2 and G-1 samples were obtained using the Siemens first derivative peak search routine; this algorithm yields fairly precise integrated intensities for resolved peaks (e.g., ±5%). Data for USW G-2 and G-1 samples employed peak intensities, and the results are not as accurate or precise as the more recent data. Precisions are listed in the appendix tables and are based on errors due to counting statistics, sample preparation, and compositional variations.

Most of our data on overlapping peaks were obtained using the first derivative routine, which divides the intensity of overlapping peaks at the midpoint between the peaks. Closely overlapping but partially resolved peaks are a problem mainly with rocks containing tridymite, cristobalite, quartz, and alkali feldspar. Overlapping peaks of these phases are now decomposed using a Gaussian peak profile, and this technique was used for data from USW WT-1 and USW WT-2. Completely overlapping peaks of mordenite and clinoptilolite or of the several alkali feldspars were not decomposed. Instead, the nonoverlapping peaks were used for estimating the abundances of mordenite and clinoptilolite. Because peaks of the alkali feldspars were chosen that are relatively insensitive to compositional changes, overlapping peaks could be used. In many tuff samples, there are at least four separate feldspar species present: groundmass and phenocryst feldspar, both of which have exsolved an additional feldspar. The resultant diffraction pattern is so complex that it is usually difficult to determine the exact nature of the individual feldspar phases.

The technique employed in our laboratory for quantitative analysis is known as the matrix-flushing method or the external standard method (Chung 1974a). This technique requires the use of reference intensities that, as Chung (1974a) pointed out, vary depending on instrumental conditions and design. We have determined the reference intensity ratios (RIR) (the ratio of the integrated intensity of a given reflection of a phase to the integrated intensity of the 113 reflection of Linde A corundum in a 1:1 mixture, by weight,) for several phases found in Yucca Mountain tuffs, but many minerals could not be isolated in pure form. Smectite from Drill Hole USW G-1 1415 was isolated by centrifugation, clinoptilolite was obtained from the Nevada Test Site in Drill Hole UE4P-1660, and quartz crystals were obtained from Hot Springs, Arkansas. The value of the RIR for calcite was taken from Chung (1974a). Calculated RIR values were used for the remaining phases, the data coming mainly from Borg and Smith (1969). Where possible, RIR values were obtained for more than one peak per phase; for example, the RIR for the quartz 100 reflection is 0.95 and the RIR for the 101 reflection is 4.32. We have recently obtained pure samples of sanidine, cristobalite, clinoptilolite, mordenite, analcime, biotite, and albite; and RIR values will be experimentally determined for all of these phases in the near future. Estimates of the percentage of glass in samples were based on the intensity of the "amorphous hump" centered on 23° 2θ, and precision is poorer for glass-containing samples than for those containing no glass.

To analyze the x-ray data, we solve the following equation, which is derived by Chung (1974b):

$$X_i = \left(\frac{k_i}{I_i} \sum_{i=1}^{n} \frac{I_i}{k_i} \right)^{-1} ,$$

where X_i is the unknown weight fraction of phase i in a mixture, k_i is the RIR for phase i, and I_i is the integrated intensity of the appropriate line of phase i. This equation is derived using the constraint that $\Sigma X_i = 1$, and the resultant equation "flushes" out the absorption coefficients by ratioing the reference intensity ratios k_i for each phase. This technique is commonly referred to as the matrix-flushing method.

Norm Calculations

To test the validity of our quantitative results, CIPW norms (Barth 1952) were calculated for a suite of samples from the devitrified Topopah Spring Member in Drill Hole USW G-1 using x-ray fluorescence analyses from Zielinsky (1983). Results of these calculations are presented in Table I, and they show that the Topopah Spring Member contains ~57 to 59% normative feldspar. This calculation is valid for comparison with the x-ray diffraction data because the devitrified Topopah Spring Member consists of ~98% feldspar plus silica polymorphs. The feldspar values in Appendix A for samples from the devitrified Topopah Spring Member agree well with the norm calculations. However, the most recent analyses for feldspar are slightly high, suggesting that the RIR for feldspar used in our analyses may be too small. This will be checked with our new standards.

Precision of Results

Quantitative x-ray diffraction traditionally yields only semiquantitative results, and, because of the problems discussed above, quantitative x-ray diffraction results will never have the high precision of typical chemical analyses. When estimating uncertainties of our determined values, errors due to peak integration, crystalline solution, sample-to-standard variability, and peak overlap were considered. Quartz has no significant crystalline solution, quartz standards should be similar to samples, and the quartz peaks are easily integrated. Our new peak-decomposition technique allows greater precision to be obtained in feldspar, cristobalite, and tridymite analyses, although feldspars exhibit exceptionally large amounts of crystalline solution and sample-to-standard variability.

TABLE I

CALCULATED CIPW NORMATIVE COMPOSITIONS OF WELDED, DEVITRIFIED PORTIONS OF THE TOPOPAH SPRING MEMBER, PAINTBRUSH TUFF

	G1-755[a]	G1-765[a]	G1-928[a]	G1-1185[a]	G1-1252[a]
SiO_2 minerals	37.3	37.5	37.7	38.5	38.1
Corundum	0.9	1.0	1.2	1.4	1.2
Orthoclase	29.3	29.4	29.4	29.1	28.7
Plagioclase	29.9	29.7	29.4	28.1	29.5
(Total Feldspar)	(59.2)	(59.2)	(58.8)	(57.2)	(58.2)
Orthopyroxene	0.4	0.4	0.4	0.8	0.6
Ilmenite	0.1	0.1	0.1	0.2	0.1
Hematite	2.1	1.8	1.8	1.9	1.8

[a]Based on x-ray fluorescence analyses reported in Zielinsky (1983). Normative compositions are reported as weight percentages for comparison to x-ray diffraction data.

III. A THREE-DIMENSIONAL INTERPRETATION OF MINERAL DISTRIBUTIONS AT YUCCA MOUNTAIN

Geologic cross sections in Appendix B show six mineral types plus glass at Yucca Mountain. These cross sections are based on recent mapping by Scott and Bonk (1984). Several drill holes shown in Fig. B-1 provide the database for these cross sections. Some of the drill holes for which x-ray data are tabulated in this report have been projected onto these cross sections (Fig. B-1) in order to make the most use of available data. Where such projections occur, an attempt was made to align the projections along the strike of major structural blocks. The only exception is the projection of UE-25b#1 directly onto the trace of Drill Hole UE-25a#1 because these drill holes are so closely spaced.

The cross sections in Appendix B show the apparent distribution of primary glass and tridymite; primary and secondary quartz; secondary smectite, clinoptilolite plus mordenite, analcime, and albite. Nearly ubiquitous minerals such as alkali feldspars and cristobalite or rare minerals such as fluorite and cryptomelane are not shown.

The basic data for this report are found in the tables of Appendix A; Appendix B is an interpretation of the tabular data in a form that is easier to visualize. Other data sources have also been used to help construct Appendix B (Bentley 1983; Bish et al. 1981; Caporuscio et al. 1982; Carroll et al. 1981; Craig et al. 1983; Levy 1984a). One cross section showing the apparent distribution of authigenic albite is based on microscope and electron microprobe analyses from Bish et al. (1982) and Caporuscio et al. (1982) rather than from the x-ray diffraction data in Appendix A. The cross sections in Appendix B are not final mineral distribution models and may be revised by new data or interpretations.

Glass

Glass occurs both above and below the potential repository host rock at Yucca Mountain (the welded devitrified Topopah Spring Member, or Tptw in Appendix B). In Appendix B, Fig. B-2, the glasses are divided into two categories, vitrophyre and nonwelded. The vitrophyre is a zone of densely welded glass at the base of the Tptw unit; this zone would first be encountered in aqueous transport downward from a repository in the overlying devitrified Tptw. The nonwelded glass occurs both above and below the Tptw unit. The nonwelded porous glass is more abundant than the vitrophyre across most of Yucca Mountain. However, the lower nonwelded vitric zone thins and disappears to the east where the stratigraphic dip and structural displacements bring the basal Tptw glassy zone closer to the static water level. The vitric nonwelded material may have important paleohydrologic significance because the preservation of open shards and pumice made of nonwelded glass is rare below past water levels (Hoover 1968). Glasses are more likely to be preserved in some dense rock types (e.g., lavas and vitrophyres) well below the static water level.

Both the vitrophyre and the nonwelded glass provide potentially reactive material at Yucca Mountain. Although glass alteration rates are generally slow, the thermal pulse of early repository history has the effect of accelerating these reactions or of thermomechanically altering the current exposure of glass to water either by fracturing the glass or by changing the movement of water. Experimental data are being sought to determine whether such effects could be significant for repository performance. The glasses are also the only rock types that retain significant amounts of ferrous iron above the deeper zones of reduced (sulfide) alteration (Caporuscio and Vaniman

1985); oxidation of the glasses' ferrous iron may be another consequence of prolonged heating, removing one of the possible barriers that could retard the transport of oxidized actinide elements.

Silica Polymorphs

The silica polymorphs, quartz, tridymite, and cristobalite are abundant throughout Yucca Mountain. Solubility and thermodynamic properties vary slightly between the silica polymorphs, and experimental studies indicate that silica concentrations in solution are controlled by cristobalite rather than quartz when both are present (Knauss et al. 1984). Tridymite will be common only in those parts of the repository workings that may extend into the middle and upper parts of the Tptw unit (Fig. B-3). Thermomechanical responses of the silica polymorphs are not anticipated to lead to any significant problems; transitions in cristobalite molar volume occur at temperatures above those anticipated near the repository.

Cristobalite is ubiquitous above the water table except in Drill Hole UE-25a#1, where cristobalite does not occur below the Tptw unit. Elsewhere cristobalite persists to depths greater than 500 m above sea level. There is a correlation between the loss of tridymite and the first appearance of abundant groundmass quartz with increasing depth. This transition takes place within the Tptw unit (Figs. B-3, B-4) and represents a major transition in the mineralogy of the proposed repository host rock (Bish et al. 1984a). This transition in part reflects the passage from zones of common high-temperature vapor-phase crystallization (tridymite) to zones of lower-temperature devitrification (quartz) within the Tptw unit.

Smectite

Previous studies have noted that smectite is a ubiquitous alteration product at Yucca Mountain, but one that is generally found in relatively small quantities (Bish et al. 1982). Although this statement is generally true, the data summarized here indicate that two zones of abundant smectite can be mapped within Yucca Mountain. These zones occur at the top of the vitric nonwelded base of the Tiva Canyon Member (lower Tpcw) that contains 7% to 35% smectite and at the top of the basal vitrophyre of the Topopah Spring Member that contains 5% to 45% smectite (Fig. B-5). The smectite intervals that can be traced through the cross sections are generally less than 1 m thick but are notably thicker in Drill Holes USW G-1, G-2, and UE-25a#1. The continuity of these two intervals is important, particularly the interval at the top of the basal vitrophyre within the Tptw unit immediately below the proposed repository horizon. The sorptive potential of this thin interval is high, and it may provide an important supplement to the more abundant zeolitized zones at greater depths. The thermal stability of this smectite zone and the probable time-temperature-hydration history of the layer under repository conditions are being studied as an important part of retardation modeling of Yucca Mountain.

In addition to these laterally continuous smectite-bearing intervals, there is also a tendency for smectites to be concentrated near some major structures. Smectite concentrations occur near Yucca Wash (USW G-2) and along Drill Hole Wash (USW G-1, UE-25a#1 and b#1). Scott et al. (1984) propose that major strike-slip faults may occur within Drill Hole Wash, and similar structures may occur along Yucca Wash. Smectite abundances are exceptionally high within the drill holes near these proposed structures, and the amount of interstratified, relatively nonsorptive illite increases with depth in these locations (Caporuscio et al. 1982). It is still uncertain how these major structures may interact with the transport pathways away from the repository.

Jones (1982) attempted to use clay-mineralogic criteria as evidence of past variations of water-table elevation in alluvium in northern Frenchman Flat, NTS. He proposed that variations in the smectite 001 spacing would reflect changes in the water-table elevation. Jones (1982) found slightly more expanded basal spacings for smectites up to 50 m above the present water table and suggested that this may be showing the effects of increased hydration, but these small changes are of doubtful statistical significance. It is well documented that smectite basal spacings are a function of the interlayer cation and the partial pressure of water in contact with the smectite (Gillery 1959; Suquet et al. 1975). Therefore, it is doubtful that these variations can be attributed uniquely to variation in paleowater-table level. The smectites in Yucca Mountain typically show no systematic trends in the 001 spacing with depth near the water table (Carroll et al. 1981; Caporuscio et al. 1982; Vaniman et al. 1984) and have basal spacings characteristic of mixed sodium-calcium interlayers. The only apparent change in phase assemblage near the water table in Yucca Mountain is the alteration of vitric tuff of Calico Hills and lower Topopah Spring Member.

Clinoptilolite and Mordenite

Previous studies have emphasized the occurrence of at least four mappable zones of clinoptilolite (or heulandite) plus mordenite zeolitization beneath Yucca Mountain (Bish et al. 1984a; Vaniman et al. 1984). There is sufficient petrologic evidence to show that these intervals occur principally where glassy material remained outside the zones of devitrification in the centers of ash flows. Therefore, there is a general correlation of zeolitized material with the nonwelded tops, bottoms, and distal edges of ash flows. This stratigraphic control is evident in Fig. B-6, but exceptions to this relationship occur (e.g., the occurrence of zeolitized tuff in the devitrified Tram Member, Tctw, of USW G-3). Indeed, the first zeolitized interval below the proposed repository horizon occurs within the densely welded Topopah Spring Member, at the boundary between the devitrified zone and the vitrophyre lithologies (compare Figs. B-2 and B-6). The origins of this particular interval may be very different from the deeper zeolite intervals (Levy 1984b); at this boundary, water was liberated at elevated temperatures during early devitrification to form heulandite in the adjacent vitrophyre. Zeolites also form in fractures crossing the devitrified intervals (Carlos 1985). These various occurrences point out the complexities of zeolite formation at Yucca Mountain and suggest multiple origins involving both closed and open systems, high and low temperatures (e.g., Moncure et al. 1981). These varieties of zeolitization will be described in future research.

The thicker zeolitized bands in Fig. B-6 tend to follow those intervals that retained glass following early tuff devitrification. This relationship allows correlation of these zeolitized intervals between drill holes where the same welded and nonwelded zones can be found. Problems with such correlations occur where some zones of greater welding pinch out (e.g., the welded Prow Pass Member or Tcpw between USW G-1 and H-5), where zones of zeolitization pinch out between drill holes, or where zones of welding have no simple anticorrelation with zeolitized intervals (compare the zeolitized and welded zones in USW G-4 and UE-25b#1, Fig. B-6). These are areas where alternate correlations between drill holes might be drawn. Future studies will address the problems of correlation.

Phillipsite and Erionite

Although phillipsite and erionite were previously reported to occur in several samples from both UE25a#1 and J-13 (Heiken and Bevier 1979; Sykes et al. 1979), we have found no evidence for the presence of these two zeolites in these samples. Heiken and Bevier (1979) reported erionite in samples JA-15, JA-32, and JA-33BC and phillipsite in JA-13 all from Drill Hole J-13. These analyses were based primarily on electron microprobe data, although the discussion of JA-32 included an XRD identification they list as "erionite(?)." Sykes et al. (1979) reported the occurrence of erionite in YM-34 from Drill Hole UE-25a#1 based on scanning electron microscope (SEM) examination.

We have reexamined all the above samples by x-ray diffraction and found no evidence for the occurrence of erionite or phillipsite (Table II). These analyses agree with those published in Carroll et al. (1981). Minimum detection limits for phases such as erionite, phillipsite, mordenite, and clinoptilolite are on the order of 1%. In addition, the x-ray patterns of these zeolites are distinctive and their identification by XRD is usually unambiguous.

There are several explanations for the previous erionite and phillipsite identifications. All of the JA erionite and phillipsite analyses relied upon electron microprobe data. It is difficult to obtain reliable chemical data for hydrous, finely intergrown materials, and distinctions between zeolites based upon analyses of such materials are suspect. Furthermore, it is possible for several different zeolites to yield similar chemical analyses, particularly erionite and mordenite. The tentative identification of erionite in YM-34 was based on the morphology observed with the SEM. However, we have observed identical morphologies in mordenite-rich tuffs containing no erionite (Caporuscio et al. 1982). Further studies have shown that erionite does occur at Yucca Mountain, although not in the samples where it was previously reported. Erionite has been positively identified as a fracture-lining mineral at the 1296 ft (395 m) depth in Drill Hole UE-25a#1.

Analcime and Albite

Few drill holes have penetrated deep enough to intersect analcime-bearing zones and fewer still are deep enough to contain secondary albite. Analcime typically first occurs at a depth of about 250 m above sea level but appears as high as 600 m above sea level in USW G-2 (Fig. B-7). The shallower occurrence of analcime in USW G-2 agrees with other evidence of major hydrothermal alteration up to the 600-m elevation (Bish and Semarge 1982). Authigenic albite has been found only in USW G-1, G-2, and UE-25b#1 (Bish et al. 1981; Caporuscio et al. 1982). Authigenic albite occurs only below 500 m above sea

TABLE II

X-RAY ANALYSIS OF JA AND YM SAMPLES

Sample	Mineral	Abundance
JA-13	Smectite	1-3%
	Mica	1-3%
	Quartz	10-20%
	Alkali Feldspar	70-90%
JA-15	Mica	1-3%
	Quartz	30-40%
	Alkali Feldspar	60-70%
JA-32	Smectite	1-3%
	Mica	2-5%
	Quartz	30-40%
	Alkali Feldspar	55-65%
JA-33	Smectite	2-4%
	Mica	2-5%
	Quartz	30-45%
	Alkali Feldspar	50-60%
YM-34	Smectite	∼5%
	Clinoptilolite	60-80%
	Mordenite	5-10%
	Quartz	5-15%
	Alkali Feldspar	5-10%

level and may generally occur at much greater depths throughout most of the exploration block. As with analcime, the shallowest occurrence of authigenic albite is in USW G-2 (1080-m depth).

IV. SUMMARY

Quantitative treatment of x-ray diffraction data provides accurate determination of mineral abundances within fine-grained rocks. This method is exceptionally useful in rocks such as tuff where the most abundant primary and secondary minerals are too fine grained for optical determination. Using this method on samples from drill holes at Yucca Mountain, mineralogic zones have been mapped in three dimensions. Both primary and secondary minerals at Yucca Mountain are subject to significant vertical variation or stratigraphic control. A thorough knowledge of where and why these variations occur will allow more reliable predictions of the mineral types that may occur along flow paths away from a repository in the Topopah Spring Member. Particularly well-constrained zonation occurs in the preservation of primary glass and in the transition from tridymite to quartz with depth. Zonation of smectite and clinoptilolite/mordenite is relatively well constrained in some intervals but may be difficult to correlate between some drill holes. The deeper alteration products, analcime and albite, are less commonly sampled and are therefore difficult to map.

ACKNOWLEDGMENTS

Thanks are due to E. Semarge and L. Maassen for help with x-ray diffraction analyses, to D. Krier for reviewing the manuscript, to R. Scott for helpful comments, and to B. Hahn for typing the manuscript.

APPENDIX A

X-RAY DIFFRACTION ANALYSIS OF TUFF FROM CORE, CUTTINGS, AND SIDEWALL SAMPLES

X-RAY DIFFRACTION ANALYSIS OF TUFF

Cuttings

Sample	Depth (m)	Smectite	Mica	Clinoptilolite	Tridymite	Quartz	Cristobalite	Alkali Feldspar	Glass	Hematite
J-12										
620-630	192.0	9±4	3±2	-	-	-	6±3	53±10	30±20	-
650-660	201.2	<1	2±1	2±1	13±4	2±1	10±3	70±10	-	<1
710-720	219.5	<1	1±1	-	<2	14±2	7±3	78±10	-	<1
770-780	237.7	1±1	-	-	-	14±2	4±2	81±10	-	<1
860-870	265.2	<1	-	-	-	10±2	4±2	86±10	-	1±1
905-915	275.8-278.9	3±2	<1	-	-	12±2	3±2	83±10	-	<1
983-992	299.6-302.4	<1	<1	-	-	24±3	8±3	68±10	-	-
1067-1077	325.2-328.3	<1	<1	-	-	34±4	3±2	63±10	-	<1
1093-1097	333.1-334.4	38±7	-	51±10	-	<1	11±3	-	-	-
1121-1126	341.7-343.2	-	-	-	-	2±1	4±2	14±5	80±20	-
1136-1139	346.3-347.2	33±7		54±10	-	2±1	10±3	-	-	-

Core

Sample	Depth (m)	Smec-tite	Mica	Clino-ptilolite	Morden-ite	Anal-cime	Quartz	Alkali Feldspar	Calcite	Kaolinite	Other
UE25b-1H											
2402	732.1	10-20	2-10	-	-	-	30-50	30-50	-	-	-
2450	746.8	5-15	5-10	-	-	-	30-50	30-50	2-10	-	-
2525	769.6	5-15	5-15	-	-	-	30-50	30-50	-	-	-
2596	791.3	5-15	2-10	-	-	-	30-50	30-50	2-10	-	-
2651	808.0	5-15	2-10	-	-	-	30-50	30-50	-	-	-
2737	834.2	2-5	2-10	-	-	-	20-40	40-60	-	-	-
2832	863.2	10-20	2-10	2-5	10-25	-	15-30	20-40	2-5	-	-
2846.7	867.7	7±3	2±1	<2	18±9	-	29±4	44±10	-	-	-
2855	870.2	10-25	2-5	2-5	10-25	-	15-30	20-40	2-10	-	-
2867	873.9	10-25	2-10	-	2-5	-	20-40	40-60	-	-	-
2879	877.5	15-30	10-20	5-15	5-15	-	20-40	20-40	2-10	-	-
2919	889.7	-	5-15	-	20-40	-	15-30	20-40	-	-	-
2946	897.9	2-10	2-10	-	-	-	30-50	30-50	2-10	-	-
2953	900.1	2-10	2-10	-	-	-	30-50	30-50	2-10	-	-
2988	910.7	5-15	5-15	TR.	-	-	30-50	30-50	2-5	-	-
3050	929.6	5-15	5-15	2-5	-	-	20-40	40-60	2-10	-	-
3092	942.4	2-10	5-10	TR.	-	-	40-60	30-50	2-5	-	-
Fracture											
3092	942.4	-	2-10	-	-	-	30-50	20-40	15-30	-	-
3095	943.4	<5	5-15	-	-	-	30-50	40-60	-	-	-
3098	944.3	5-15	5-15	-	-	-	20-40	40-60	2-5	-	-
3128	953.4	5-15	5-15	-	-	-	20-40	40-60	2-5	-	-
Fracture											
3128	953.4	2-5	2-5	-	-	-	20-40	20-40	15-30	-	-
3163	964.1	2-5	5-15	-	-	-	20-40	40-60	2-5	-	-
Fracture											
3163	964.1	-	2-5	-	-	-	10-30	10-30	50-70	-	-
3185	970.8	10-25	10-20	-	-	-	20-40	30-50	-	-	-
Fracture											
3185	970.8	<5	<5	-	-	-	5-15	-	60-80	-	2-10[A], 10-30[B]
3196	974.1	2-10	5-15	-	-	-	20-40	40-60	-	-	-
3222	982.1	2-5	5-15	-	-	-	20-40	50-70	-	-	-
3225	983.0	5-15	5-15	-	-	-	20-40	40-60	-	-	-
3257	992.7	30-50	5-15	-	-	-	10-30	20-40	-	-	-
3267	995.8	15-30	2-10	-	-	-	30-50	20-40	-	-	-
3298	1005.2	5-15	2-10	-	-	Tr.	20-40	40-60	-	-	-
3326	1013.8	5-15	5-15	-	-	2-5	20-40	40-60	-	-	-
3362	1024.7	10-25	5-15	-	-	2-5	20-40	30-50	-	Tr.	-
3374	1028.4	5-15	5-15	-	-	10-30	20-40	20-40	-	<2	-
3393	1034.2	5-15	5-10	-	-	10-30	20-40	20-40	5-15	2-5	-
3401	1036.6	2-5	2-10	-	-	10-30	20-40	20-40	2-5	2-5	-
3459	1054.3	5-15	5-15	-	-	10-30	20-40	15-30	2-10	2-10	-

APPENDIX A (cont)

Core (cont)

Sample	(m)	Smec-tite	Mica	Clino-ptilolite	Morden-ite	Anal-cime	Quartz	Alkali Feldspar	Calcite	Kaolinite	Other
UE25b-1H											
3469	1057.4	5-15	5-15	-	-	10-30	20-40	20-40	2-10	2-10	-
3506	1068.6	10-25	5-15	-	-	10-30	20-40	20-40	2-10	2-10	-
3530	1075.9	10-20	5-10	-	-	15-30	20-40	30-50	<5	<2	-
Fracture											
3530	1075.9	10-20	-	-	-	5-15	20-40	20-40	-	5-10	-
3548	1081.4	5-15	5-15	-	-	2-5	20-40	30-50	2-10	2-5	-
Inclusion											
3548	1081.4	10-20	5-15	-	-	-	15-30	30-50	10-20	<2	-
3571	1088.4	5-10	2-10	-	-	2-5	30-50	15-30	20-40	<5	-
3572	1088.7	2-10	2-10	-	-	<2	20-40	30-50	15-30	<2	-
Inclusion											
3572	1088.7	10-25	5-15	-	-	-	20-40	20-40	5-15	<2	-
3602	1097.9	5-15	2-10	-	-	10-30	20-40	20-40	5-15	<2	-
Fracture											
3602	1097.9	<5	-	-	-	5-15	2-10	-	30-50	-	30-50[a]
3660	1115.6	5-15	2-10			15-30	20-40	20-40	2-10	2-5	-
Fracture											
3660	1115.6	-	-	-	-	15-30	10-20	2-10	50-70	-	-
3708	1130.2	5-15	2-10	-	-	-	25-45	40-60	-	2-5	-
3767	1148.2	5-15	5-15	-	-	15-30	25-45	15-30	5-15	2-10	-
3792	1155.8	10-20	5-10	-	-	5-15	20-40	30-50	2-10	2-5	-
3835	1168.9	10-20	5-10	-	-	15-30	20-40	20-40	2-10	2-5	-
3880	1182.6	10-20	5-10	-	-	10-20	20-40	20-40	5-15	2-5	-
3901	1189.0	30-50	2-10	-	-	Tr.	20-40	15-30	-	Tr.	-
3902	1189.3	30-50	2-5	-	2-10	-	15-30	15-30	15-30	-	-
3904	1189.9	20-40	-	-	-	15-30	20-40	15-30	2-5	-	-
3910	1191.8	5-15	-	-	-	2-10	30-50	30-50	-	-	-
3926	1196.6	10-20	5-15	-	-	-	20-40	20-40	10-20	2-10	-
3956	1205.8	15-30	5-15	-	-	2-5	15-30	30-50	2-10	2-5	-
3963	1207.9	20-40	5-15	-	-	10-25	20-40	20-40	2-10	Tr.	-
3988	1215.5	10-25	10-25	-	-	-	20-40	30-50	-	-	-
Fracture											
3988	1215.5	2-5	2-5	-	-	-	5-15	10-20	70-90	-	-

[a] Fluorite

[b] Todorokite

Core

Sample	Depth (m)	Smectite	Mica	Clinoptilolite	Mordenite	Analcime	Quartz	Cristobalite	Alkali Feldspar	Calcite	Other
USW G-2											
10	3.0	-	5-10	-	-	-	-	30-50	30-50	-	10-20[a]
100	30.5	-	<5	-	-	-	-	30-50	30-50	-	10-25[a]
200	61.0	-	-	-	-	-	-	30-50	30-50		5-15[a]
230	70.1	-	-	-	-	-	-	30-50	30-50	-	5-15[a]
270	82.3	2-10	-	-	-	-	-	30-50	30-50	15-30	-
304	92.7	-	-	-	-	-	5-10	30-50	30-50	-	10-20[a]
331	100.9	30-50	-	-	-	-	-	-	30-50	10-20	-
338	103.0	40-60	-	-	-	-	-	-	5-10	-	30-50[b]
358	109.1	15-30	-	-	-	-	Tr.	5-10	20-40	-	20-40[b]
395	120.4	5-15	<2	-	-	-	<5	10-20	15-30	-	30-50[b]
501	152.7	5-20	<3	-	-	-	-	5-10	10-20	-	40-60[b]
547	166.7	5-15	<5	-	-	-	-	5-15	10-20	-	40-60[b]
548	167.0	-	<5	5-10	-	-	-	20-40	30-50	-	-
561	171.0	10-20	<3	10-20	-	-	-	20-40	25-40	-	-
627	191.1	5-15	<5	10-20	-	-	-	20-40	30-50	-	-
675	205.7	30-50	<5	15-30	-	-	-	5-10	15-30	-	-
723	220.4	5-15	<5	-	-	-	-	<5	5-10	30-50	15-30[b]
743	226.5	30-50	<5	<5	-	-	5-15	5-15	10-20	5-15	15-30[b]
762	232.3	2-5	-	75-90	-	-	-	5-15	<5	-	10-20[a]
770	234.7	<2	5-10	-	-	-	-	15-30	60-80	-	-
822	250.5	5-10	<5	-	-	-	-	20-40	30-50	-	10-20[a]
855	260.6	<5	2-5	-	-	-	-	20-40	30-50	-	5-15[a]
898	273.7	<2	2-5	<5	-	-	-	20-40	40-60	-	5-10[a]
921	280.7	10-20	-	-	-	-	20-40	15-30	20-40	5-10	-
951	289.9	<2	-	-	-	-	15-30	20-40	20-40	-	-
984	299.9	2-10	-	-	-	-	15-30	10-20	15-30	15-30	-
1032	314.6	2-10	<2	-	-	-	15-30	20-40	20-40	-	-
1072	326.7	2-10	<2	-	-	-	20-40	5-15	30-50	-	-
1133	345.3	5-15	<2	-	-	-	15-30	20-40	40-60	-	-
1178	359.1	<5	<2	-	-	-	10-25	20-40	30-50	-	-
1234	376.1	2-10	-	-	-	-	10-25	20-40	30-50	-	-
1281	390.4	5-15	-	-	-	-	15-30	15-30	30-50	-	-
1331	405.7	5-15	-	-	-	-	15-30	20-40	30-50	-	-
1382	421.2	5-15	<2	-	-	-	15-30	15-30	40-60	-	-
1420	432.8	5-15	-	-	-	-	15-30	20-40	30-50	-	-
1461	445.3	5-15	-	-	-	-	10-20	30-50	30-50	-	-
1536	468.2	10-20	-	<5	-	-	10-20	30-50	30-50	-	-
1585	483.1	5-15	-	<5	-	-	10-25	20-40	30-50	-	-
1634	498.0	30-50	<2	30-50	-	-	-	15-30	-	-	-
1664	507.2	<2	-	<2	-	-	5-10	5-10	10-20	-	50-70[b]
1691	515.4	5-15	-	40-60	5-10	-	-	15-25	5-15	-	-
1745	531.9	10-20	-	30-50	5-10	-	5-10	15-30	10-20	-	-
1752	534.0	5-15	-	50-70	5-10	-	<5	5-15	5-10	-	-
1798	548.0	<2	-	40-60	15-30	-	5-15	10-20	15-30	-	-
1848	563.3	-	-	40-60	15-30	-	Tr.	15-30	10-20	-	-
1899	578.8	<2	<2	40-60	15-30	-	5-10	10-20	10-20	-	-
1952	595.0	-	<5	5-10	40-60	-	10-20	10-20	10-20	-	-
2001	609.9	-	<2	5-10	40-60	-	10-20	10-20	15-30	-	-

APPENDIX A (cont)

Core (cont)

Sample	Depth (m)	Smec-tite	Mica	Clino-ptilolite	Morden-ite	Anal-cime	Quartz	Cristo-balite	Alkali Feldspar	Calcite	Other
USW G-2											
2078	633.4	<5	<5	20-40	20-40	-	5-10	10-20	10-20	-	-
2158	657.8	<5	<5	20-40	15-30	Tr.	5-10	15-30	10-20	-	-
2248	685.2	<5	<2	20-40	20-40	-	5-15	15-30	15-30	-	-
2353	717.2	<2	2-10	5-15	20-40	-	15-30	15-30	10-20	-	-
2430	740.7	<5	5-15	20-40	5-15	-	20-40	0-10	20-40	-	-
2528	770.5	<5	5-15	<5	15-30	-	20-40	<5	20-40	-	-
2667	812.9	<5	5-10	-	20-40	-	15-30	<5	30-50	-	-
2744	836.4	<5	<2	-	-	-	30-50	5-10	40-60	-	-
2820	859.5	<2	<2	-	-	-	20-40	2-10	50-70	-	-
2869	874.5	<2	2-5	-	-	-	20-40	2-5	50-70	-	-
2887	880.0	<5	<2	-	-	-	20-40	2-5	50-70	-	-
2950	899.2	2-10	<3	-	-	-	20-40	2-10	40-60	-	-
2970	905.3	5-15	<3	-	-	-	30-50	0-10	40-60	-	-
3037	925.7	30-50	<2	-	<5	-	20-40	0-5	15-30	-	-
3067	934.8	-	<2	5-10	20-40	-	-	20-40	20-40	-	-
3192	972.9	5-10	-	20-40	5-15	Tr.	20-40	0-5	20-40	-	-
3250	990.6	15-30	<2	5-15	5-15	20-40	15-30	0-5	15-30	-	-
3308	1008.3	2-5	10-20	-	-	-	15-30	0-10	40-60	-	-
3330	1015.0	-	2-10	-	-	-	20-40	0-10	50-70	-	-
Fracture											
3330	1015.0	5-15	2-10	-	-	-	10-20	-	15-30	-	40-60[e]
3349	1020.8	<2	2-10	-	-	-	15-30	0-10	50-70	-	-
3366	1026.0	<2	2-10	-	-	-	20-40	0-10	50-70	-	-
3416	1041.2	<2	2-10	-	-	-	20-40	-	50-70	-	-
3454	1052.8	20-35	<5	-	15-30	Tr.	15-35	-	15-35	-	-
3492	1064.4	10-25	<5	-	15-30	5-10	20-40	-	15-30	-	-
3512	1070.5	10-20	5-10	-	2-10	10-20	20-40	-	30-50	-	<5[c]
3541	1079.3	5-15	5-10	-	-	20-40	20-40	-	15-30	-	<5[c]
3578	1090.6	15-30	5-15	-	15-30	-	20-40	-	15-30	-	-
3627	1105.5	10-20	5-15	-	-	<5	20-40	-	30-50	-	-
3671	1118.9	5-15	5-10	-	-	5-10	20-40	-	30-50	5-10	<2[c]
3720	1133.9	5-15	5-10	-	-	Tr.	20-40	-	30-50	-	-
3724	1135.1	20-30	<5	-	-	-	30-50	-	20-40	-	<5[c]
3750	1143.0	20-30	5-15	-	-	-	20-40	-	30-50	-	-
3772	1149.7	15-30	5-10	-	-	-	20-40	-	30-50	-	-
3795	1156.7	25-40	-	-	-	<2	30-50	-	20-40	-	<5[c]
3833	1168.3	20-40	2-10	-	-	-	20-40	-	20-40	-	-
3875	1181.1	20-30	5-10	-	-	<5	30-50	-	15-30	-	-
3908	1191.2	10-25	-	-	-	-	20-40	-	30-50	2-10	-
3933	1198.8	10-20	-	-	-	20-40	20-40	-	20-40	5-10	-
3968	1209.4	10-25	2-10	-	-	Tr.	30-50	-	30-50	-	Tr.[c]
4005	1220.7	10-20	5-15	-	-	<5	15-30	-	30-50	5-10	-
4090	1246.6	15-30	10-25	-	-	2-10	15-30	-	20-40	5-15	-
4167	1270.1	10-20	10-20	-	-	<2	15-30	-	30-50	5-15	<5[c]
4199	1279.9	10-20	5-15	-	-	Tr.	10-25	-	30-50	10-25	<2[c]
4209	1282.9	5-15	5-10	-	-	2-10	10-25	-	40-60	<5	-
4267	1300.6	10-20	5-10	-	-	<5	20-40	-	30-50	<5	-
4329	1319.5	5-15	2-10	-	-	<5	20-40	-	30-50	5-15	-

Core (cont)

Sample	Depth (m)	Smec-tite	Mica	Clino-ptilolite	Morden-ite	Anal-cime	Quartz	Cristo-balite	Alkali Feldspar	Calcite	Other
USW G-2											
Pumice											
4467	1361.5	15-30	-	-	-	-	15-30	-	30-50	5-15	-
4467	1361.5	5-15	2-10	-	-	<5	15-30	-	30-50	5-15	-
4570	1392.9	5-15	5-10	-	-	<5	20-40	-	30-50	10-25	-
4788	1459.4	10-20	<5	-	-	Tr.	20-40	-	30-50	5-15	-
4805	1464.6	10-30	-	-	-	Tr.	30-50	-	30-50	-	-
4816	1467.9	15-30	-	-	-	Tr.	30-50	-	20-40	2-10	-
4838	1474.6	15-30	-	-	-	<5	20-40	-	30-50	2-10	-
4873	1485.3	20-40	-	-	-	<2	20-40	-	20-40	-	-
4885	1488.9	20-40	-	-	-	-	20-40	-	20-40	<5	-
4893	1491.4	15-30	5-10	-	-	<2	20-40	-	20-40	-	-
4924	1500.8	10-25	5-15	-	-	<5	20-40	-	20-40	5-10	-
4949	1508.5	30-50	5-15	-	-	-	15-30	-	15-30	-	-
5017	1529.2	10-30	-	-	-	-	20-40	-	30-50	-	<5[c]
Spherulite											
5017	1529.2	2-10	-	-	-	-	30-50	-	30-50	2-10	<5[c]
5029	1532.8	10-30	10-30	-	-	-	20-40	-	20-40	-	-
5144	1567.9	2-10	10-30	-	-	-	20-40	-	30-50	2-10	-
5171	1576.1	10-25	20-40	-	-	-	15-30	-	15-30	2-10	-
5206	1586.8	10-20	10-25	-	-	Tr.	15-30	-	30-50	-	2-10[c]
5213	1588.9	5-15	5-15	-	-	-	20-40	-	20-40	2-10	5-15[c]
5305	1617.0	5-15	5-15	-	-	-	15-30	-	30-50	5-15	<2[c]
5369	1636.5	5-15	10-20	-	-	-	20-40	-	30-50	5-15	-
5379	1639.5	2-10	10-20	-	-	-	20-40	-	30-50	5-15	-
5434	1656.3	2-10	15-30	-	-	<2	15-30	-	30-50	-	-
5493	1674.3	<5	15-30	-	-	-	20-40	-	30-50	10-20	-
5505	1677.9	5-15	10-20	-	-	-	15-30	-	30-50	5-10	2-10[d]
5538	1688.[illegible]	15-35	-	-	-	-	15-30	-	20-40	10-25	5-15[d]
5596	1705.7	10-20	-	-	-	-	15-30	-	30-50	2-10	5-10[d]
5638	1718.5	10-25	-	-	-	Tr.	10-25	-	30-50	10-25	2-10[d]
5657	1724.3	20-40	-	-	-	-	15-30	-	20-40	2-10	2-10[d]
5696	1736.1	10-20	-	-	-	<2	15-30	-	30-50	10-25	5-15[d]
5762	1756.3	5-15	-	-	-	-	15-30	-	30-50	15-30	5-15[d]
5820	1773.9	-	-	-	-	-	15-30	-	30-50	2-10	10-25[d]
5885	1793.7	10-25	-	-	-	-	15-30	-	10-25	20-40	2-10[d]
5895	1796.8	10-25	-	-	-	-	20-40	-	20-40	15-30	2-10[d]
5918	1803.8	5-15	-	-	-	-	30-50	-	30-50	-	2-10[c],2-5[d]
5926	1806.2	10-20	-	-	-	Tr.	30-50	-	30-50	-	-
5931	1807.8	15-30	-	-	-	-	15-30	-	30-50	2-10	5-15[c]
5951	1813.9	15-30	-	-	-	<2	20-40	-	30-50	2-10	<5[c]
5971	1820.0	10-25	-	-	-	<5	20-40	-	30-50	-	-
5992	1826.4	10-25	-	-	-	<5	30-50	-	30-50	2-10	<5[c]

[a] Tridymite
[b] Glass
[c] Kaolinite
[d] Chlorite
[e] Hematite

Core (cont)

Sample	Depth (m)	Smectite	Mica	Clinoptilolite	Analcime	Quartz	Cristobalite	Tridymite	Alkali Feldspar	Calcite	Glass	Other
USW GU-3												
31.0	9.5	2-4	1-3	-	-	-	5-15	-	70-80	10-15	-	-
45.0	13.7	-	-	-	-	-	15-20	4-8	70-80	-	-	-
79.0	24.1	-		-	-	1-3	4-8	20-30	65-75	-	-	-
103.1	31.4	-	-	-	-	1-3	15-25	5-10	65-75	1-3	-	-
Fracture		-	-	-	-	-	1-3	1-3	6-12	85-95	-	-
196.3	59.8	-	-	-	-	-	20-30	-	70-80	-	-	-
Vein		2-4	-	-	-	-	2-5	-	5-15	80-90	-	-
245.7	74.9	1-3	-	-	-	1-3	20-30	2-4	65-75	-	-	-
303.6	92.5	<1	-	-	-	-	20-30	-	70-80	-	-	-
316.8	96.6	-	-	-	-	-	20-25	-	70-80	-	-	-
341.5	104.1	2-5	-	-	-	-	25-35	-	65-75	-	-	-
356.5	108.7	5-10	-	-	-	-	10-20	-	35-45	-	30-50	-
376.1	114.6	3-6	-	-	-	2-4	2-8	-	45-55	-	30-50	-
410.0	125.0	16-24	<1	-	-	1-3	20-30	-	45-55	-	-	-
414.3	126.3	2-5	<1	-	-	2-5	15-25	-	70-80	-	-	-
417.5	127.3	10-15	<1	-	-	4-8	15-20	-	60-70	-	-	-
424.4	129.4	-	-	-	-	1-3	15-20	4-8	70-80	-	-	-
429.0	130.8	-	1-3	-	-	2-6	15-25	2-6	65-75	-	-	-
Vein		-	-	-	-	-	1-3	-	4-8	90-95	-	-
430.5	131.2	-	2-4	-	-	-	10-15	2-6	75-85	-	-	-
465.5	141.9	-	<1	-	-	-	6-12	5-15	75-85	-	-	-
482.0	146.9	-	<1	-	-	-	5-10	15-25	65-75	2-4	-	-
520.3	158.6	-	-	-	-	-	2-8	15-25	65-75	2-4	-	-
Cavity		-	-	-	-	-	-	10-20	10-15	75-80	-	-
525.3	160.1	-	-	-	-	<1	4-8	15-25	65-75	-	-	-
579.0	176.5	<1	-	-	-	-	20-25	10-15	60-70	-	-	-
633.4	193.1	<1	<1	-	-	1-3	20-25	5-10	65-75	-	-	-
674.7	205.7	<1	<1	-	-	1-3	20-25	2-8	65-75	-	-	-
Fracture		-	-	-	-	10-15	-	60-80	15-20	-	-	-
702.5	214.1	<1	<1	-	-	4-8	15-20	-	65-75	-	-	-
769.1	234.4	<1	<1	-	-	<1	20-25	2-10	60-70	-	-	-
849.4	258.9	<1	<1	-	-	2-6	15-20	-	70-80	-	-	-
Fracture		-	-	-	-	75-80	<1	2-8	10-20	-	-	-
910.5	277.5	<1	-	-	-	2-6	25-30	-	60-70	-	-	-
Fracture		<1	-	-	-	15-20	1-3	30-50	35-45	-	-	-
924.3	281.7	<1	-	-	-	10-15	10-15	5-15	60-70	-	-	-
Fracture		-	-	-	-	75-85	<1	10-15	5-10	-	-	-
951.1	289.9	<1	-	-	-	6-10	15-20	2-8	65-75	-	-	-
954.8	291.0	<1	<1	-	-	15-20	10-15	-	65-75	-	-	-
1027.0	313.0	-	-	-	-	2-10	15-20	-	70-80	-	-	-
Fracture		1-3	-	-	-	5-9	<1	-	4-8	35-45	-	35-45[a]
1061.0	323.4	-	-	-	-	18-22	5-10	-	65-75	-	-	-
1130.3	344.5	-	<1	-	-	15-20	8-12	-	65-75	-	-	-
1175.0	358.1	<1	<1	-	-	30-40	2-4	-	55-65	-	-	-
1195.7	364.5	4-6	-	-	-	2-4	25-30	-	30-40	-	20-40	-
Vein		-	-	<1	-	6-10	20-25	-	65-75	-	-	-
1227.0	374.0	1-3	-	-	-	6-10	15-20	-	30-40	-	30-50	-
1302.4	397.0	1-3	-	-	-	2-6	10-15	-	35-45	-	30-60	-
1322.0	403.0	-	-	-	-	2-6	4-10	-	25-35	-	50-80	-
1344.8	409.9	-	-	-	-	5-10	5-10	-	25-35	-	40-70	-
1369.6	417.5	-	-	-	-	2-6	2-10	-	20-30	-	50-80	-
1394.5	425.0	-	-	-	-	2-6	2-10	-	25-35	-	50-80	-
1394.6	425.1	-	-	-	-	2-6	2-10	-	25-35	-	50-80	-

APPENDIX A (cont)

Core (cont)

Sample	Depth (m)	Smectite	Mica	Clinoptilolite	Analcime	Quartz	Cristobalite	Tridymite	Alkali Feldspar	Calcite	Glass	Other
USW GU-3												
1415.5	431.4	-	-	-	-	2-8	2-10	-	30-40	-	40-70	-
1439.2	438.7	-	-	-	-	15-25	2-10	-	15-25	-	40-70	-
1439.5	438.8	<1	1-3	-	-	2-8	2-10	-	30-40	-	40-70	-
1468.5	447.6	-	1-3	-	-	2-8	2-10	-	30-40	-	40-70	-
1493.7	455.3	<1	-	1-3	-	2-8	2-10	-	20-30	-	50-80	-
1498.3	456.7	-	-	2-4	-	4-10	2-10	-	20-30	-	50-80	-
1510.7	460.5	2-4	<1	-	-	2-8	2-10	-	20-30	-	50-80	-
1537.5	468.6	2-4	2-4	1-3	-	15-20	2-6	-	45-55	2-4	10-30	1-3[b]
1571.6	479.0	1-3	1-3	-	-	2-6	2-8	-	40-50	-	30-60	-
1598.5	487.2	3-6	<1	-	-	2-8	1-3	-	40-50	-	30-60	-
1603.0	488.6	-	<1	-	-	1-3	25-35	-	60-70	-	-	-
1624.2	495.1	-	-	-	-	15-25	1-3	5-10	65-75	-	-	-
1653.2	504.0	<1	<1	-	-	10-20	1-5	10-20	65-75	-	-	-
1709.0	521.0	<1	-	-	-	10-15	10-15	-	65-75	1-3	-	-
1744.0	531.6	-	-	-	-	4-8	20-30	-	65-75	-	-	-
1827.2	557.0	-	-	15-25	-	2-6	2-6	-	65-75	-	-	-
1874.0	571.2	-	-	45-55	-	5-10	2-8	-	35-45	-	-	-
1935.8	590.0	2-5	-	55-65	-	2-6	2-6	-	25-35	-	-	-
1986.0	605.3	-	-	65-75	-	2-6	4-8	-	15-25	-	-	-
1993.1	607.5	-	-	55-65	-	2-6	8-12	-	20-30	-	-	-
2013.2	613.6	1-3	1-3	45-55	-	2-4	2-6	-	35-45	-	-	-
Fracture		25-35	2-4	10-20	-	5-15	-	-	35-45	-	-	-
2070.2	631.0	1-3	-	-	-	15-25	2-4	5-10	65-75	-	-	-
2138.2	651.7	1-3	1-3	-	-	15-20	10-15	-	65-75	-	-	Tr[b]
2177.3	663.6	1-3	1-3	-	-	16-24	6-14	-	60-70	-	-	Tr[b]
2189.3	667.3	1-3	1-3	-	-	10-15	12-18	-	65-75	-	-	Tr[b]
2198.0	670.0	1-3	1-3	-	-	10-15	15-20	-	65-75	-	-	-
2226.0	678.5	98-100	-	-	-	-	-	-	-	-	-	1-2[c]
2360.0	719.3	-	1-3	-	-	17-23	10-15	-	65-75	-	-	1-2[b]
Fracture		1-3	1-3	-	-	35-40	-	-	35-45	-	-	10-25[d]
2369.4	722.2	1-3	1-3	-	-	15-20	10-15	-	65-75	-	-	1-2[b]
2467.4	752.1	-	1-3	-	-	18-22	8-12	-	65-75	-	-	1-2[b]
2548.4	776.8	25-35	1-3	10-15	-	6-10	-	-	45-55	-	-	-
2577.4	785.6	2-4	4-8	45-55	-	1-3	2-8	-	30-40	-	-	1-2[b]
2615.3	797.1	1-3	2-6	35-45	-	3-7	5-10	-	40-50	-	-	-
2623.4	799.6	2-4	1-3	25-35	-	3-7	1-4	-	55-65	-	-	-
2656.6	809.7	2-6	3-7	25-35	-	3-7	6-10	-	45-55	-	-	-
2695.7	821.7	<1	2-4	25-35	-	5-10	5-15	-	35-45	-	-	5-15[d]
Fracture		-	<1	5-15	-	75-85	5-15	-	-	-	-	5-15[d]
2727.4	831.3	1-2	2-4	-	-	15-20	10-20	-	60-70	-	-	-
2914.5	888.3	-	2-4	-	-	18-24	5-10	-	60-70	-	-	-
2971.0	905.6	1-2	2-5	-	-	12-18	10-15	-	65-75	-	-	-
3004.5	915.8	-	2-5	-	-	25-35	2-6	-	60-70	-	-	-
Fracture		-	3-6	-	-	15-20	1-3	-	70-80	-	-	-
3045.3	928.2	1-2	2-4	-	-	18-24	5-10	-	60-70	-	-	-
3113.1	948.9	1-2	3-6	-	-	10-15	15-20	-	60-70	-	-	-
3164.1	964.4	1-3	3-6	5-15	-	6-12	10-20	-	55-65	-	-	-
3207.4	977.6	1-3	2-4	5-15	-	6-12	15-20	-	55-65	-	-	-
Fracture		3-5	5-7	10-20	-	14-18	10-20	-	40-50	-	-	-
3226.0	983.3	4-6	2-4	2-10	-	10-15	10-20	-	55-65	-	-	-
3239.0	987.3	-	1-3	-	-	14-18	10-20	-	60-70	-	-	-

Core (cont)

Sample	Depth (m)	Smec- tite	Mica	Clino- ptilolite	Anal- cime	Quartz	Cristo- balite	Tridy- mite	Alkali Feldspar	Calcite	Glass	Other
USW GU-3												
Fracture		-	1-3	-	-	30-35	8-15	-	50-60	-	-	2-10[e]
3311.0	1009.2	2-4	2-4	10-20	-	12-16	5-15	-	50-60	-	-	-
3475.3	1059.3	2-4	3-5	15-25	-	12-16	5-15	-	45-55	-	-	-
3589.4	1094.1	5-10	2-5	30-40	-	10-15	4-10	-	30-40	-	-	-
3672.0	1119.2	4-8	2-5	10-20	-	14-18	4-12	-	40-50	-	-	4-10[d]
3759.1	1145.8	6-12	2-6	10-20	-	25-30	-	-	40-50	-	-	-
3854.8	1174.9	5-10	1-3	30-40	-	20-30	-	-	25-35	-	-	-
3859.3	1176.3	2-4	1-3	20-30	-	25-30	-	-	35-45	4-6	-	-
3936.3	1199.8	1-2	4-6	5-15	2-8	28-32	<1	-	45-55	-	-	-
4008.3	1221.7	2-4	5-8	-	10-20	30-35	-	-	40-50	-	-	-
4117.0	1254.9	2-6	<1	-	6-12	32-38	-	-	45-55	-	-	-
4240.6	1292.5	10-15	2-4	-	-	25-30	-	-	45-55	5-10	-	-
4263.8	1299.6	2-6	1-3	-	20-30	30-35	-	-	30-40	1-2	-	-
4297.1	1309.8											
Fractur		2-6	1-2	-	5-10	35-40	-	-	5-10	35-45	-	-
4416.0	1346.0	2-6	1-2	-	5-10	35-40	-	-	6-12	35-45	-	-
4423.0	1348.1	6-12	1-3	10-15	5-10	30-35	-	-	30-40	1-3	-	-
4503.7	1372.7	15-25	1-3	2-6	2-6	35-40	-	-	30-40	-	-	-
Fracture		5-10	1-2	2-4	-	60-65	-	-	25-35	-	-	-
4568.4	1392.5	15-20	2-4	1-3	10-15	25-30	-	-	30-40	1-2	-	-
4600.3	1402.2	4-8	1-3	1-3	-	48-54	-	-	35-45	-	-	-
4708.5	1435.2	6-12	1-3	-	15-20	32-36	-	-	30-40	1-3	-	-
4756.5	1449.8	4-8	1-3	-	10-15	35-40	-	-	35-45	-	-	-
4786.4	1458.9	5-10	1-3	-	15-20	30-35	-	-	35-45	-	-	-
4803.2	1464.0	1-2	1-3	-	15-20	32-38	-	-	35-45	-	-	-
4869.4	1484.2	2-4	1-2	-	35-40	32-36	-	-	20-30	-	-	-
4906.5	1495.5	1-3	1-3	-	30-40	32-36	-	-	25-30	-	-	-
5014.0	1528.3	2-6	1-3	-	10-20	35-40	-	-	35-45	-	-	-

[a] Fluorite
[b] Hornblende
[c] Hematite
[d] Mordenite
[e] Cryptomelane

APPENDIX A (cont)

Core (cont)

Sample	Depth (m)	Smec-tite	Mica	Clino-ptilolite	Morden-ite	Quartz	Cristo-balite	Alkali Feldspar	Tridy-mite	Glass	Other
USW G-4											
47	14.3	2±1	-	-	-	2±1	28±5	70±10	-	-	-
72	21.9	<1	-	-	-	2±1	28±5	70±10	-	-	-
107	32.6	-	-	-	-	2±1	32±5	67±10	-	-	-
143	37.5	30±10	-	-	-	-	21±5	49±10	-	-	-
148	45.1	35±15		-	-	-	15±10	-	-	50±20	-
170	51.8	28±10	5±2	-	-	8±2	5±2	40±20	-	20±10	-
220	67.1	10±5	3±2	-	-	4±2	5±2	60±20	-	20±10	-
231	70.4	8±4	10±5	-	-	-	3±2	60±20	-	20±10	-
236	71.9	-	-	-	-	10±5	10±5	20±10	-	60±20	-
268	81.7	-	<1	-	-	-	6±2	73±10	20±10	-	-
280	85.3	-	<1	-	-	-	5±2	80±20	10±5	-	-
332	101.2	-	2±1	-	-	-	15±5	76±20	7±5	-	-
383	116.7	3±2	<1	-	-	-	11±5	70±10	15±10	-	-
410	125.0	3±2	<1	-	-	<1	12±5	66±10	17±10	-	-
416	126.8	3±2	<1	-	-	<1	14±5	73±10	9±5	-	-
447	136.2	2±1	<1	-	-	3±1	20±5	68±10	6±4	-	-
514	156.7	2±1	-	-	-	2±1	22±5	69±10	6±4	-	-
556	169.5	2±1	-	-	-	8±2	9±5	58±10	19±10	-	-
625	190.5	2±1	-	-	-	17±4	6±2	63±10	11±5	-	-
676	206.0	3±1	-	-	-	4±1	23±5	66±10	4±2	-	-
694	211.5	3±2	-	-	-	4±1	13±2	62±10	17±8	-	-
746	227.4	<1	-	-	-	3±1	28±5	68±10	-	-	-
817	249.0	2±1	-	-	-	25±3	7±3	65±10	-	-	-
934	284.7	<1	-	-	-	16±2	11±4	63±10	8±4	-	-
1026	312.7	<1	-	-	-	9±2	20±5	66±10	5±2	-	-
1089	331.9	<1	-	-	-	12±2	10±4	61±10	16±8	-	-
1089, Fracture	331.9	-	-	-	-	66±5	<1	32±10	-	-	-
1117	340.5	<1	-	-	-	16±2	14±4	69±10	-	-	-
1163	354.5	-	-	-	-	16±2	15±4	69±10	-	-	-
1163, Inclusion	354.5	<1	-	-	-	35±5	3±2	61±10	-	-	-
1190	362.7	<1	-	-	-	25±3	13±4	60±10	-	-	-
1244	379.2	<1	<1	-	-	17±3	15±4	67±10	-	-	-
1282	390.8	<1	<1	-	-	16±3	18±4	65±10	-	-	-
1283-1293E	391.1-394.1	<1	<1	-	-	6±2	23±4	69±10	-	-	-
1299	395.9	2±1	-	5±2	-	8±2	23±4	62±10	-	-	-
1301	396.5	<1	<1	5±2	-	9±2	20±4	65±10	-	-	-
1310	399.3	<1	<1	3±2	-	5±2	24±5	65±10	-	-	-
1314	400.5	45±10	-	28±5	-	2±1	14±4	11±5	-	-	-
1330	405.4	-	-	-	-	10±5	-	20±10	-	70±20	-
1341	408.7	-	-	-	10±5	-	30±10	-	60±20	-	-
1372	418.2	6±2	2±1	1±1	-	5±2	12±5	36±10	-	40±20	-
1381	420.9	7±3	-	56±10	-	5±2	4±2	28±10	-	-	-
1381, Inclusion	420.9	4±2	10±5	-	10±5	-	-	-	-	75±20	-
1392	424.3	2±1	-	75±15	-	2±1	4±2	21±10	-	-	-
1392,	424.3	-	2±1	-	-	5±3	-	-	-	95±20	-

Core (cont)

Sample	Depth (m)	Smectite	Mica	Clinoptilolite	Mordenite	Quartz	Cristobalite	Alkali Feldspar	Tridymite	Glass	Other
USW G-4											
Inclusion											
1419	432.5	-	2±1	30±10	-	7±2	8±3	53±10	-	-	-
1432	436.5	3±2	4±2	75±15	-	11±4	7±4	-	-	-	-
1438	438.3	3±2	<1	75±15	-	4±2	4±2	13±5	-	-	-
1470	448.1	3±2	-	77±10	-	6±2	14±4	-	-	-	-
1544	470.6	3±2	-	50±10	20±10	6±2	12±4	-	-	-	-
1602	488.3	-	<1	40±10	12±5	5±2	8±4	30±10	-	-	-
1685	513.6	<1	-	50±10	15±10	4±2	7±3	19±10	-	-	-
1707	520.3	<1	<1	25±10	12±5	3±2	14±4	38±10	-	-	-
1734	528.5	-	6±2	30±10	10±5	12±2	15±4	29±10	-	-	-
1763	537.4	7±3	-	50±10	-	-	32±5	13±5	-	-	-
1779	542.2	2±1		45±10	-	-	10±4	44±10	-	-	-
1788	545.0	3±1	-	28±10	-	4±2	5±2	51±10	-	-	-
1788, Fracture	545.0	-	-	-	93±10	7±2	-	-	-	-	-
1794	546.8	-	<1	-	-	3±1	29±5	67±10	-	-	-
1841	561.1	2±1	<1	-	-	27±5	3±2	67±10	-	-	-
1871	570.3	<1	<1	-	-	23±5	5±2	69±10	-	-	-
1938	590.7	<1	-	-	-	5±2	29±4	65±10	-	-	-
1952	595.0	<1	-	-	-	5±2	18±4	76±10	-	-	-
1968	599.8	3±2	-	15±5	20±10	8±2	10±4	45±10	-	-	-
1989	606.2	-	<1	44±10	-	7±3	15±4	33±10	-	-	-
2039	621.5	-	-	30±10	15±10	5±2	8±3	42±10	-	-	-
2069	630.6	-	-	35±10	20±10	3±1	4±2	35±10	-	-	-
2090	637.0	-	-	10±5	35±10	5±2	10±4	40±10	-	-	-
2100	640.1	2±1	-	30±10	30±10	2±1	-	35±10	-	-	-
2100, Fracture	640.1	-	-	5±3	35±10	20±4	-	40±10	-	-	-
2131	649.5	-	<1	30±10	20±10	2±1	-	46±10	-	-	-
2202	671.2	-	-	40±10	10±5	4±2	7±3	37±10	-	-	-
2226	678.5	<1	-	35±10	15±10	6±2	2±1	38±10	-	-	-
2236	682.1	<1	-	50±10	25±10	6±2	-	18±10	-	-	-
2263	689.8	-	5±3	-	-	19±5	<1	75±10	-	-	-
2285	696.5	<1	5±3	-	-	32±5	2±1	60±10	-	-	-
2343	714.1	<1	3±2	-	-	31±5	-	65±10	-	-	-
2343, Fracture 1	714.1	9±5	3±2	-	-	49±5	-	39±10	-	-	-
2343, Fracture 2	714.1	6±3	2±1	-	-	38±5	-	54±10	-	-	-
2355	717.8	-	3±1	-	-	31±5	-	66±10	-	-	-
2381	725.7	<1	2±1	-	-	30±5	-	67±10	-	-	-
2423	738.5	<1	2±1	-	-	26±5	-	70±10	-	-	-
2516	766.9	-	3±1	-	-	29±5	-	68±10	-	-	-
2533	772.1	<1	2±1	-	-	31±5	-	66±10	-	-	-
2551	777.5	-	2±1	-	-	25±5	-	73±10	-	-	-
2566	782.1	-	2±1	-	-	31±5	-	68±10	-	-	-
2598	791.9	<1	2±1	-	-	25±5	-	71±10	-	-	-
2681	817.2	22±5	2±1	-	-	9±4	-	67±10	-	-	-

Core (cont)

Sample	Depth (m)	Smec-tite	Mica	Clino-ptilolite	Morden-ite	Quartz	Cristo-balite	Alkali Feldspar	Tridy-mite	Glass	Other
USW G-4											
2716	827.8	-	-	-	80±10	20±5	-	-	-	-	-
2731	832.4	-	-	13±5	60±10	27±5	-	-	-	-	-
2754	839.4	12±5	2±1	23±10	-	29±5	-	33±10	-	-	-
2758	840.6	-	5±2	3±2	15±5	24±5	-	53±10	-	-	-
2762	841.9	<1	6±2	3±2	15±5	23±5	-	52±10	-	-	-
2792	851.0	9±2	4±2	70±15	17±5	-	-	-	-	-	-
2823	860.5	2±1	6±2	16±10	8±5	28±5	-	39±10	-	-	-
2823, Fracture	860.5	7±5	2±1	5±3	60±20	27±5	-	-	-	-	-
2840	865.6	-	6±2	-	-	39±5	-	54±10	-	-	-
2875	876.3	-	4±2	-	-	35±5	-	61±10	-	-	-
2947	898.2	-	3±2	-	-	31±5	-	66±10	-	-	-
2947, Fracture	898.2	-	-	-	-	10±5	-	-	-	-	80±20[a]
3000	914.4	-	4±2	-	-	42±5	-	54±10	-	-	-

[a] Cryptomelane

Sidewall and Cuttings*

Sample	Depth (m)	Smec-tite	Mica	Heulandite-Clinoptilolite	Morden-ite	Tridy-mite	Quartz	Cristoba-lite	Alkali Feldspar	Glass	Horn-blende
USW-H3											
1550(SW)	472.4	trace	0-1	0-5	-	5-10	5-15	5-10	60-80	-	-
1655(SW)	504.5	trace	0-1	0-5	-	5-10	5-10	5-10	65-85	-	-
1700(SW)	518.2	trace	0-1	0-5	-	-	5-15	10-20	50-70	10-20	-
1800(SW)	548.6	0-5	0-1	50-70	-	-	5-10	-	20-40	-	-
1900(SW)	579.1	5-10	0-1	70-80	-	0-5	0-5	0-5	10-20	-	
2400(SW)	731.5	-	0-1	70-80	-	-	0-5	0-5	10-20	-	0-1
2440(SW)	743.7	-	0-1	30-40	20-40	-	0-5	0-5	20-40	-	-
2490(SW)	759.0	0-5	0-2	40-50	20-30	-	0-5	-	10-30	-	-
USW-H4											
1312(SW)	399.9	0-5	0-1	0-10	-	-	5-15	5-10	20-40	50-70	-
1420(SW)	432.8	0-5	0-1	60-80	-	-	0-5	0-5	20-30	-	-
1455(SW)	443.5	-	0-1	40-50	20-30	-	0-5	0-5	10-30	-	-
1550(SW)	472.4	0-5	-	65-85	-	-	0-2	0-5	10-20	-	-
1656(SW)	504.8	-	-	-	-	-	0-5	20-50	50-80	-	-
USW-H5											
50(DC)	15.2	-	-	-	-	10-25	-	0-5	70-90	-	-
190(DC)	57.9	-	-	-	-	0-5	-	20-30	70-90	-	-
420(DC)	128.0	10-20	-	-	-	-	0-2	10-15	30-40	40-50	0-1
450(DC)	137.2	-	-	-	-	-	0-2	-	0-5	95-98	-
700(DC)	213.4	trace	0-1	-	-	15-25	-	10-20	55-75	-	-
1050(DC)	320.0	trace	0-1	-	-	-	0-5	30-50	45-65	-	-
1610(DC)	490.7	-	-	-	-	-	0-2	0-5	5-10	85-95	-
1666(SW)	507.8	40-60	-	5-15	-	-	0-2	10-15	20-30	-	-
1750(DC)	533.4	-	-	trace?	-	-	0-5	0-10	0-10	80-90	-
1762(SW)	537.1	-	-	-	-	-	0-2	0-2	0-10	90-100	-
1800(SW)	548.6	-	0-1	-	-	-	0-5	0-5	5-15	80-90	-
1852(SW)	564.5	-	0-1	-	-	-	0-5	-	5-10	90-100	-
1875(SW)	571.5	-	-	trace?	-	-	0-5	trace?	0-10	90-95	-
1917(SW)	584.3	-	0-1	20-30	-	-	25-35	10-20	25-45	-	-
1930(DC)	588.3	0-5	0-2	40-60	-	-	10-20	-	25-35	-	-
1966(SW)	599.2	0-10	-	-	-	-	0-5	-	10-20	65-85	-
2200(DC)	670.6	trace	-	50-70	-	-	0-5	0-5	30-40	-	-

*Sample numbers represent depth of sample in feet. SW = sidewall core sample. DC = drill (bit) cutting sample. Depth is only approximate for DC samples.
All data from Levy (1984a).

APPENDIX A (cont)

Cuttings

Sample	Depth (m)	Smec-tite	Mica	Tridy-mite	Quartz	Cristo-balite	Alkali Feldspar	Glass	Hematite
USW H-3									
470-480	143.3-146.3	-	2±1	13±6	-	8±3	77±10	-	1±1
520-530	158.5-161.5	-	-	Tr.	-	24±5	76±10	-	-
540-550	164.6-167.6	-	Tr.	21±4	-	5±3	73±10	-	1±1
610-620	185.9-189.0	-	-	Tr.	-	29±5	71±10	-	1±1
740-750	225.6-228.6	~1	~1	-	4±2	26±5	68±10	-	-
800-810	243.8-246.9	2±1	~1	Tr.	2±1	27±5	69±10	-	-
870-880	265.2-268.2	~1	Tr.	-	29±4	3±2	66±10	-	-
930-940	283.5-286.5	~1	~1	-	14±3	16±4	69±10	-	1±1
990-1000	301.8-304.8	~1	-	4±2	Tr.	23±5	72±10	-	-
1030-1040	313.9-317.0	~1	-	Tr.	3±1	24±5	72±10	-	1±1
1100-1110	335.3-338.3	~1	-	Tr.	2±1	23±5	74±10	-	1±1
1160-1170	353.6-356.6	~1	~1	-	2±1	29±5	67±10	-	-
1270-1280	387.1-390.1	-	2±1	-	2±1	7±4	19±10	70±20	-
1320-1330	402.3-405.4	-	-	-	2±1	5±3	23±10	70±20	-

Cuttings

Sample	Depth (m)	Smec-tite	Mica	Clino-ptilolite	Morden-ite	Tridy-mite	Quartz	Cristo-balite	Alkali Feldspar	Amphi-bole	Glass	Hema-tite
USW H-4												
310-320	94.5-97.5	-	~1	-	-	-	11±4	-	10±4	75±10	-	1±1
390-400	118.9-121.9	2±2	~1	-	-	14±4	2±1	13±4	68±10	-	-	-
440-450	134.1-137.2	2±2	-	-	-	19±5	2±1	13±4	64±10	-	-	1±1
490-500	149.4-152.4	2±2	-	-	-	11±4	~1	18±5	67±10	-	-	1±1
640-650	195.1-198.1	2±2	-	-	-	-	4±2	26±5	68±10	-	-	-
830-840	253.0-256.0	3±2	~1	-	-	12±4	~1	14±4	68±10	-	-	-
910-920	277.4-280.4	~1	-	-	-	-	11±2	20±5	67±10	-	-	-
940-950	286.5-289.6	~1	-	-	-	-	7±2	21±5	71±10	-	-	-
1040-1050	317.0-320.0	~1	-	-	-	-	6±2	23±5	70±10	-	-	-
1150-1160	350.5-353.6	2±2	~1	-	-	-	15±2	18±5	64±10	-	-	-
1190-1200	362.7-365.8	-	-	5±5	-	-	-	15±10	15±10	-	70±20	-
1230-1240	374.9-378.0	20±10	2±1	-	-	-	4±2	20±5	25±10	-	30±20	-
1320-1330	402.3-405.4	-	~1	-	-	-	31±4	9±4	59±10	-	-	-
1350-1360	411.5-414.5	-	-	78±10	-	-	3±2	9±4	10±5	-	-	-
1410-1420	429.8-432.8	-	-	52±10	-	-	7±2	9±4	31±10	-	-	-
1540-1550	469.4-472.4	3±2	-	29±10	16±5	-	11±3	10±4	31±10	-	-	-
1600-1610	487.7-490.7	-	9±3	31±10	-	-	17±4	9±4	35±10	-	-	-
1640-1650	499.9-502.9	-	-	10±5	-	-	6±2	24±5	60±10	-	-	-
1710-1720	521.2-524.3	~1	~1	-	-	-	33±5	3±2	61±10	-	-	1±1
1790-1800	545.6-548.6	3±2	-	-	-	-	15±4	17±5	64±10	-	-	-
1900-1910	579.1-582.2	-	~1	22±7	-	-	5±2	16±10	56±10	2±2	-	-
1980-1990	603.5-606.6	3±2	11±5	23±6	-	2±1	6±3	55±10	2±2	-	-	-

Cuttings

Sample	Depth (m)	Smec-tite	Mica	Clino-ptilolite	Tridy-mite	Quartz	Cristo-balite	Alkali Feldspar	Hematite
USW H-5									
720-730	219.5-222.5	3±2	Tr.	-	23±10	-	9±5	65±10	1±1
800-810	243.8-246.9	3±2	-	-	Tr.	2±1	24±5	72±10	1±1
830-840	253.0-256.0	-	-	-	Tr.	-	24±5	76±10	1±1
920-930	280.[illegible]-283.5	2±2	<1	-	Tr.	3±1	24±5	71±10	-
970-980	295.7-298.7	2±2	-	-	Tr.	2±1	26±5	71±10	1±1
1150-1160	350.5-353.6	2±2	Tr.	-	-	26±5	10±5	62±10	1±1
1230-1240	374.9-378.0	2±2	Tr.	-	-	7±2	23±5	69±10	-
1290-1300	393.2-396.2	2±2	<1	-	-	10±2	18±5	71±10	1±1
1380-1390	420.6-423.7	2±2	<1	-	-	15±4	20±5	65±10	1±1
1450-1460	442.0-445.0	Tr.	<1	-	-	20±5	8±5	71±10	-
1490-1500	454.2-457.2	2±2	<1	-	-	9±2	21±5	68±10	1±1
1590-1600	484.6-487.7	35±10	-	10±5	-	-	17±5	40±10	-
1710-1720	521.2-524.3	3±2	-	-	-	5±3	5±3	20±10	70±20

Core

Sample	Depth (m)	Smec-tite	Mica	Clino-ptilolite	Anal-cime	Quartz	Cristo-balite	Alkali Feldspar	Glass	Other
USW H-6										
1092.4	333.0	trace	trace	-	-	20±5	9±5	70±10	-	-
1128.8	344.1	trace	<1	-	-	21±5	12±5	66±10	-	-
1149.2	350.3	trace	trace	-	-	16±5	15±5	69±10	-	-
1166.3	355.5	3±2	<1	-	-	21±5	13±5	62±10	-	-
1368.4	417.1	10±5	trace	-	-	20±5	8±5	60±10	60±25	-
1376.2	419.5	trace	2±1	-	-	10±5	11±5	60±10	60±25	-
1380.8	420.9	10±5	-	-	-	7±5	10±5	20±10	60±25	-
1426.6	434.8	-	<1	6±3	-	7±5	10±5	25±10	60±25	-
1511.7	460.8	10±5	2±1	36±5	-	7±5	-	49±10	10±5	-
1671.4	509.4	trace	trace	-	-	5±3	23±5	72±10	-	-
1679.2	511.8	-	trace	-	-	4±2	25±5	72±10	-	-
1829.5	557.6	-	2±1	-	-	21±5	6±5	71±10	-	-
2051.0	625.1	trace	4±2	-	-	20±5	8±5	68±10	-	trace[a]
2354.6	717.7	-	2±1	-	-	17±5	13±5	67±10	-	-
2865.0	873.3	trace	3±2	18±5	-	29±5	-	50±10	-	-
3003.2	915.4	-	15±5	26±5	-	-	5±3	51±10	-	3±2[a]
3188.4	971.8	3±2	12±5	-	-	5±3	19±5	63±10	-	2±1[a]
3605.2	1098.9	trace	10±5	3±2	-	5±3	7±5	58±10	15±10	2±1[a]
3806.0	1160.1	3±2	8±5	9±5	12±5	22±5	2±1	46±10	-	-

Notes: (a) hornblende, (-) not detected.

APPENDIX A (cont)

Cuttings

Sample	Depth (m)	Smectite	Mica	Clinoptilolite	Mordenite	Tridymite	Quartz	Cristobalite	Alkali Feldspar	Calcite	Glass	Hematite
USW WT-1												
440-450	134.1-137.2	5±3	-	-	-	8±4	-	4±2	12±4	-	70±20	-
500-510	152.4-155.4	-	4±2	-	-	11±5	-	12±4	72±10	2±1	-	1±1
550-560	167.6-170.7	-	1±1	-	-	19±4	-	10±3	71±10	-	-	1±1
640-650	195.1-198.1	1±1	-	-	-	11±4	-	16±3	62±10	-	-	1±1
690-700	210.3-213.4	1±1	-	-	-	-	19±2	19±3	61±10	-	-	1±1
780-790	237.7-240.8	1±1	-	-	-	3±2	25±3	9±2	61±10	1±1	-	-
840-850	256.0-259.1	1±1	1±1	-	-	6±3	20±2	16±3	56±10	-	-	<1
930-940	283.5-286.5	1±1	-	-	5±2	26±3	7±2	57±10	-	-	-	<1
1000-1010	304.8-307.8	1±1	-	-	-	-	22±2	16±3	60±10	1±1	-	<1
1090-1100	332.2-335.3	1±1	-	-	-	-	24±3	15±3	58±10	-	-	<1
1160-1170	353.6-356.6	1±1	-	1±1	-	-	10±2	18±3	58±10	1±1	-	<1
1220-1230	371.9-374.9	-	1±1	-	-	-	27±3	8±2	59±10	-	-	<1
1300-1310	396.2-399.3	1±1	-	2±1	-	-	35±4	4±2	59±10	-	-	<1
1320-1330	402.3-405.4	2±1	1±1	14±4	-	-	20±2	13±4	50±10	-	-	-
1340-1350	408.4-411.5	-	1±1	29±8	-	-	10±2	9±3	51±10	-	-	-
1380-1390	420.6-423.7	-	1±1	40±10	12±4	-	8±2	7±3	31±6	-	-	-
1410-1420	429.8-432.8	-	-	40±10	8±3	-	3±2	8±3	40±8	-	-	-
1470-1480	448.1-451.1	-	1±1	25±8	18±5	-	10±3	7±3	39±8	-	-	-
1510-1520	460.2-463.3	-	1±1	43±10	10±4	-	8±3	5±2	33±7	-	-	-
1550-1560	472.4-475.5	-	1±1	40±10	12±4	-	14±3	7±3	26±5	-	-	-
1570-1580	478.5-481.6	-	1±1	5±3	3±2	-	26±3	9±3	57±10	-	-	<1

APPENDIX A (cont)

Cuttings

Sample	Depth (m)	Smectite	Mica	Clinoptilolite	Mordenite	Tridymite	Quartz	Cristobalite	Alkali Feldspar	Calcite	Glass	Hematite
USW WT-2												
250-260	76.2-79.2	4±2	-	-	-	-	2±1	11±4	34±10	-	50±20	-
260-270	79.2-82.3	7±3	3±2	-	-	-	1±1	7±3	51±10	-	30±20	<1
290-300	88.4-91.4	1±1	2±1	-	-	10±4	-	9±3	78±10	-	-	1±1
420-450	128.0-131.0	1±1	<1	-	-	12±4	2±1	11±3	73±10	2±1	-	1±1
510-520	155.4-158.5	1±1	1±1	-	-	13±4	3±1	21±3	62±10	1±1	-	<1
570-580	173.7-176.8	3±2	<1	-	-	13±4	5±2	21±3	59±10	-	-	<1
650-660	198.1-201.1	2±1	<1	-	-	10±4	6±2	22±3	58±10	-	-	1±1
720-730	219.5-222.5	1±1	<1	-	-	10±4	8±2	19±3	61±10	-	-	-
780-790	237.7-240.8	1±1	<1	-	-	6±3	21±3	10±3	59±10	3±1	-	<1
850-860	259.1-262.1	1±1	<1	-	-	13±4	14±3	16±3	56±10	-	-	<1
930-940	283.5-286.5	1±1	<1	-	-	13±4	11±2	17±3	57±10	-	-	<1
990-1000	301.8-304.8	2±1	<1	-	-	-	14±2	21±3	62±10	1±1	-	<1
1060-1070	323.1-326.1	3±1	<1	-	-	-	16±2	19±3	61±10	-	-	<1
1130-1140	344.4-347.5	<1	<1	-	-	-	13±2	15±3	70±10	<1	-	<1
1190-1200	362.7-365.8	-	<1	1±1	-	-	4±3	9±3	56±10	-	30±20	-
1200-1210	365.8-368.8	1±1	-	1±1	-	-	7±4	15±4	26±10	-	50±20	-
1250-1260	381.0-384.0	2±1	1±1	-	-	-	9±4	12±4	36±10	-	40±20	-
1300-1310	396.2-399.3	-	<1	1±1	-	-	10±4	12±4	36±10	-	40±20	-
1360-1370	414.5-417.6	-	<1	<1	-	-	11±4	8±4	40±10	-	40±20	-
1420-1430	432.8-435.9	<1	<1	4±2	-	-	11±4	4±2	50±10	-	30±20	-
1450-1460	442.0-445.0	1±1	<1	<1	-	-	14±3	8±4	44±10	<1	30±20	-
1470-1480	448.1-451.1	<1	<1	5±3	-	-	8±3	8±4	49±10	-	30±20	-
1520-1530	463.3-466.3	3±2	1±1	24±5	-	-	11±3	12±4	48±10	-	-	-
1570-1580	478.5-481.6	-	2±1	19±4	-	-	18±2	7±3	53±10	-	-	-
1640-1650	499.9-502.9	1±1	<1	2±1	-	-	22±3	7±3	67±10	-	-	<1
1710-1720	521.2-524.3	1±1	<1	<1	-	-	22±3	7±3	69±10	-	-	<1
1750-1760	533.4-536.4	1±1	1±1	1±1	-	-	14±2	17±3	66±10	-	-	<1
1820-1830	554.7-557.8	4±2	-	19±4	-	-	5±2	14±3	59±10	-	-	-
1910-1920	582.2-585.2	-	1±1	42±10	-	-	5±2	6±3	47±10	-	-	-
2000-2010	609.6-612.6	-	-	30±8	10±4	-	3±2	3±2	55±10	-	-	-
2050.25	624.9	-	1±1	3±1	-	-	-	18±2	9±2	69±10	-	<1
2053.7	626.0	1±1	3±1	-	-	-	19±2	10±2	67±10	-	-	<1
2059.3	627.7	<1	3±1	-	-	-	21±2	9±2	66±10	-	-	<1

APPENDIX B

MINERALOGIC CROSS SECTIONS OF YUCCA MOUNTAIN

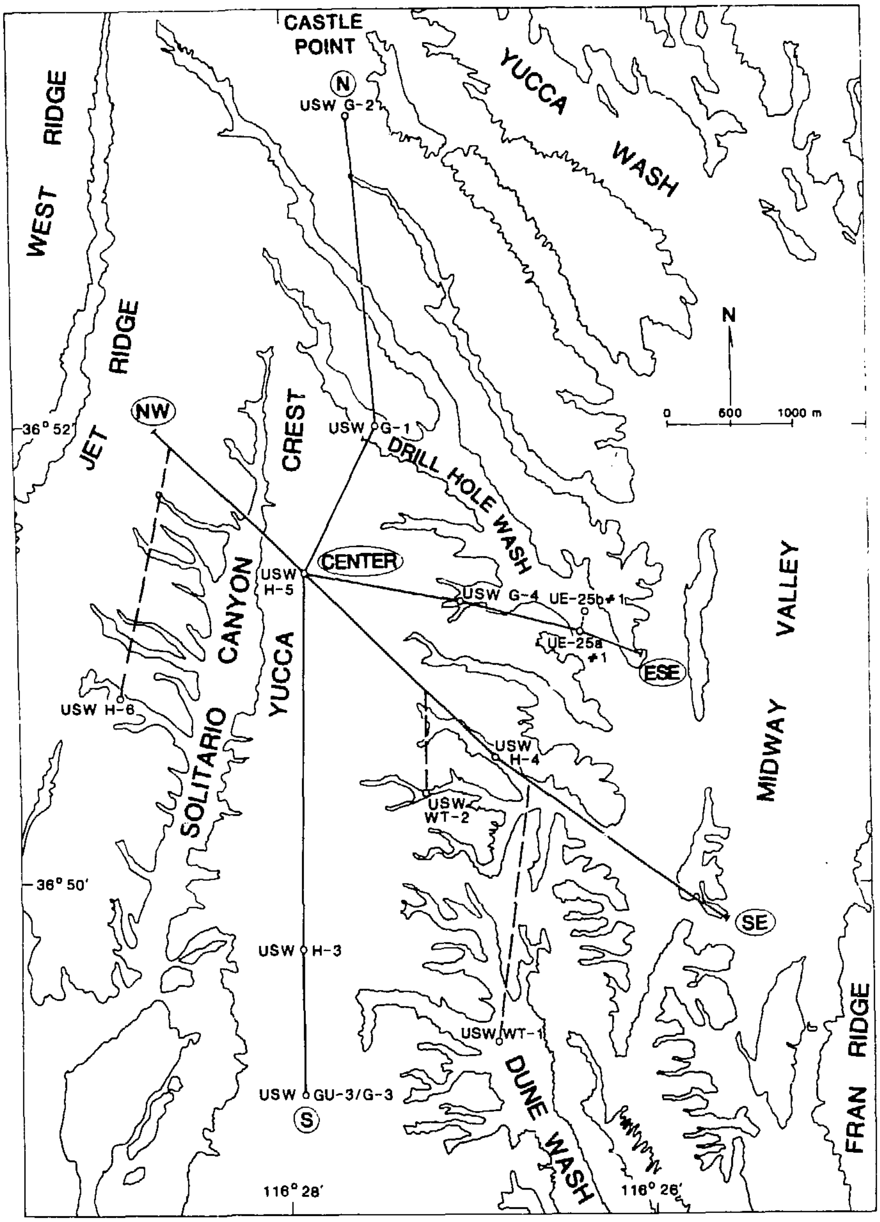

Fig. B-1.

Plan view of the Yucca Mountain area based on the map by Scott and Bonk (1984). Locations of drill holes described in this report are indicated, along with the orientations of cross-sections used in Figs. B-2 through B-8. Drill hole J-12 is located outside of this figure but can be found in the location map published by Bish et al. (1984). Figures B-2 through B-8 show mineralogy overlain on the geologic cross-sections drawn by Scott and Bonk. Several drill holes (USW H-6, WT-1, WT-2, and UE-25b#1) are projected onto the Scott and Bonk cross sections as shown.

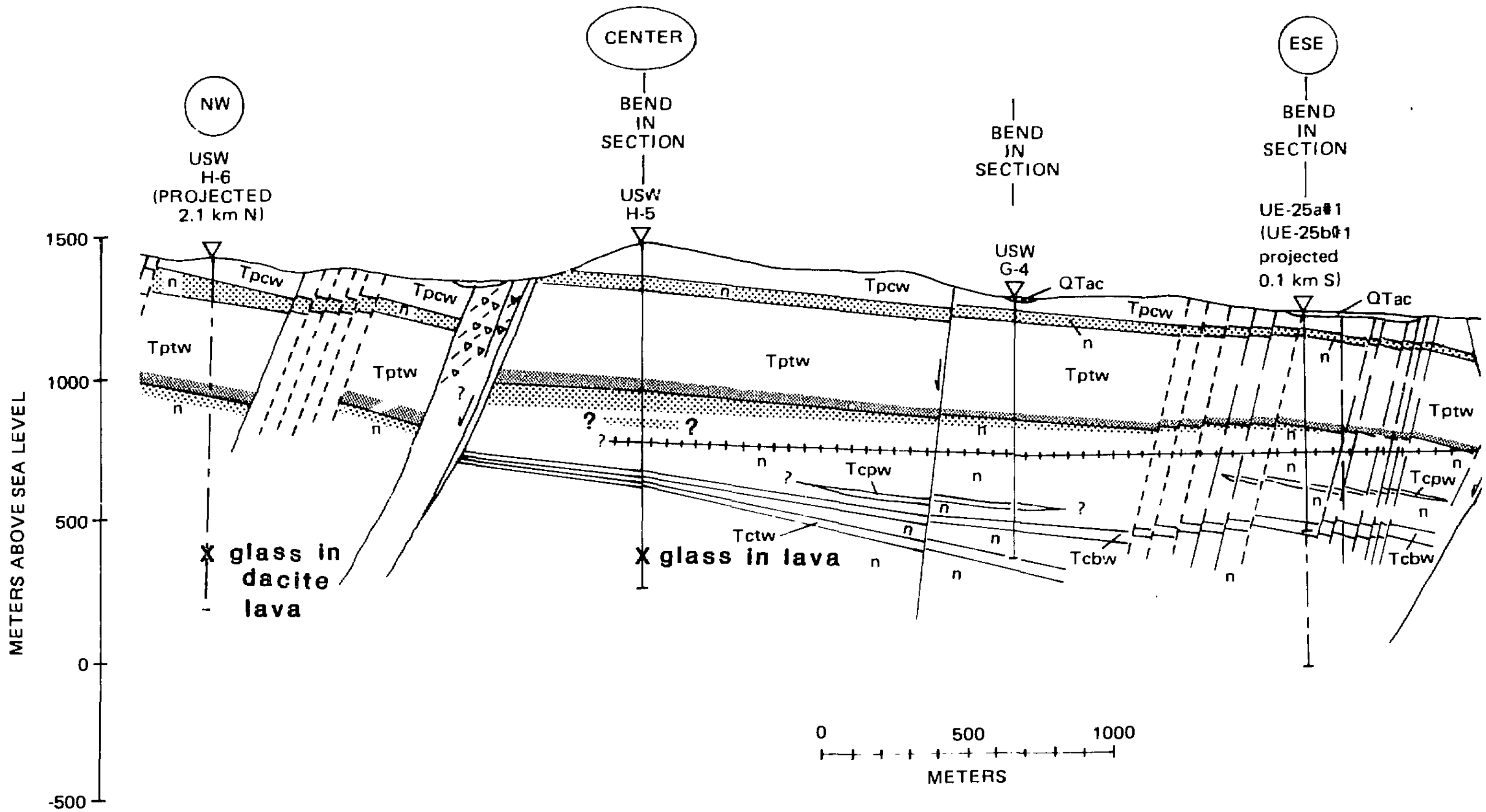

■ = vitrophyre ▒ = vitric nonwelded

Fig. B-2.

Distribution of vitrophyre (densely welded glass) and vitric nonwelded glass. Bold "X" indicates glass preserved within lava flows. In this and in the following figures, unit designations follow the usage of Scott and Bonk (1984). Tpcw, Tpyw, Tppw, and Tptw represent the welded zones of the Tiva, Yucca, Pah, and Topopah Members of the Paintbrush Tuff; Tcpw, Tcbw, and Tctw represent the welded zones of the Prow Pass, Bullfrog, and Tram Members of the Crater Flat Tuff; Tfb represents lavas and flow breccias; and Totw represents the welded zones of older tuffs. The symbol *n* is used for all nonwelded tuff zones. The subhorizontal barred line indicates the static water level.

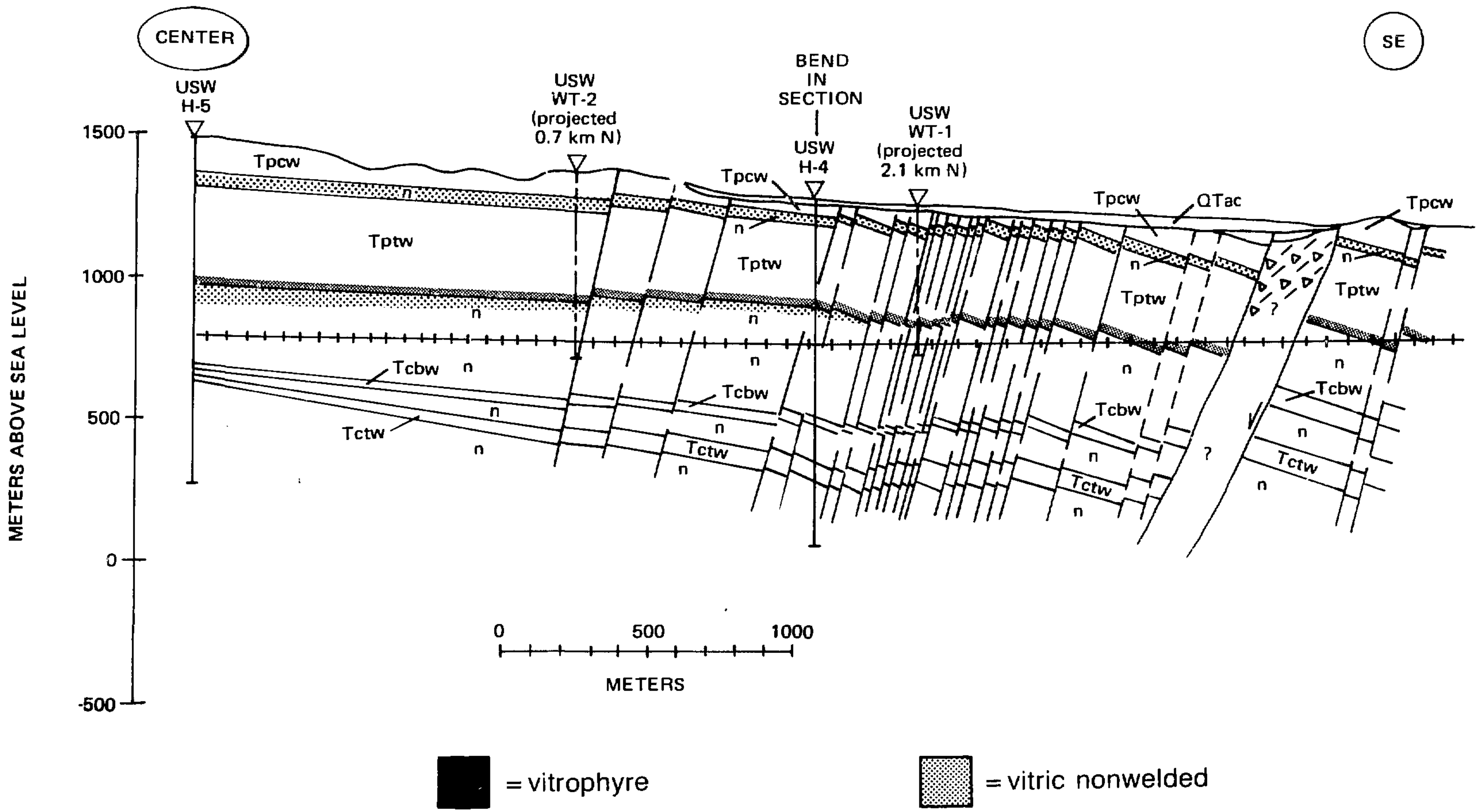
CENTER
SE
USW
H-5
USW
WT-2
(projected
0.7 km N)
BEND
IN
SECTION
USW
H-4
USW
WT-1
(projected
2.1 km N)
Tpcw
Tptw
Tcbw
Tctw
QTac
n
?
METERS ABOVE SEA LEVEL
1500
1000
500
0
-500
0
500
1000
METERS
= vitrophyre
= vitric nonwelded

Fig. B-2 (cont)

APPENDIX B (cont)

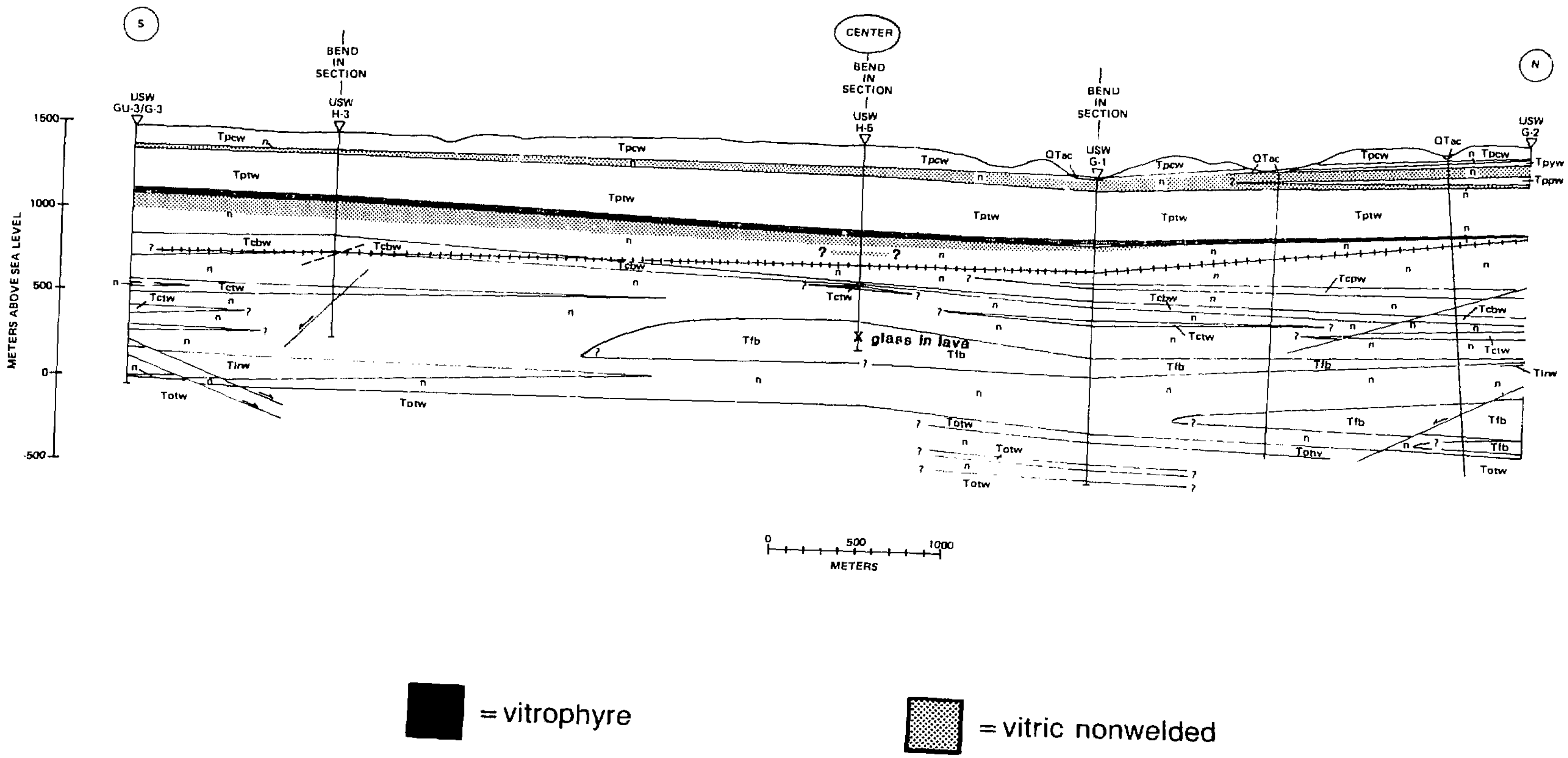

Fig. B-2 (cont)

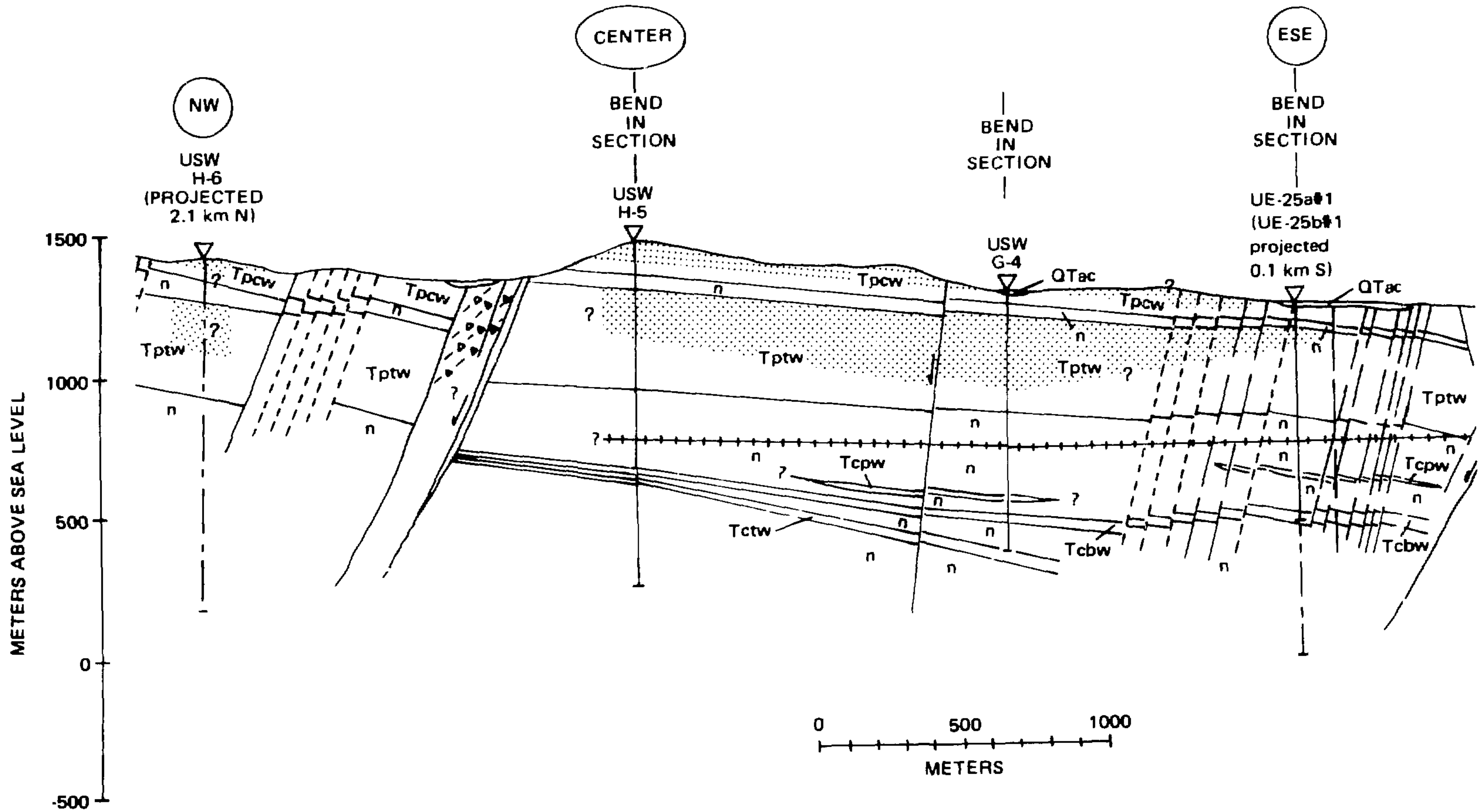

Tridymite

Fig. B-3.
Distribution of tridymite. Symbols are defined in Fig. B-2.

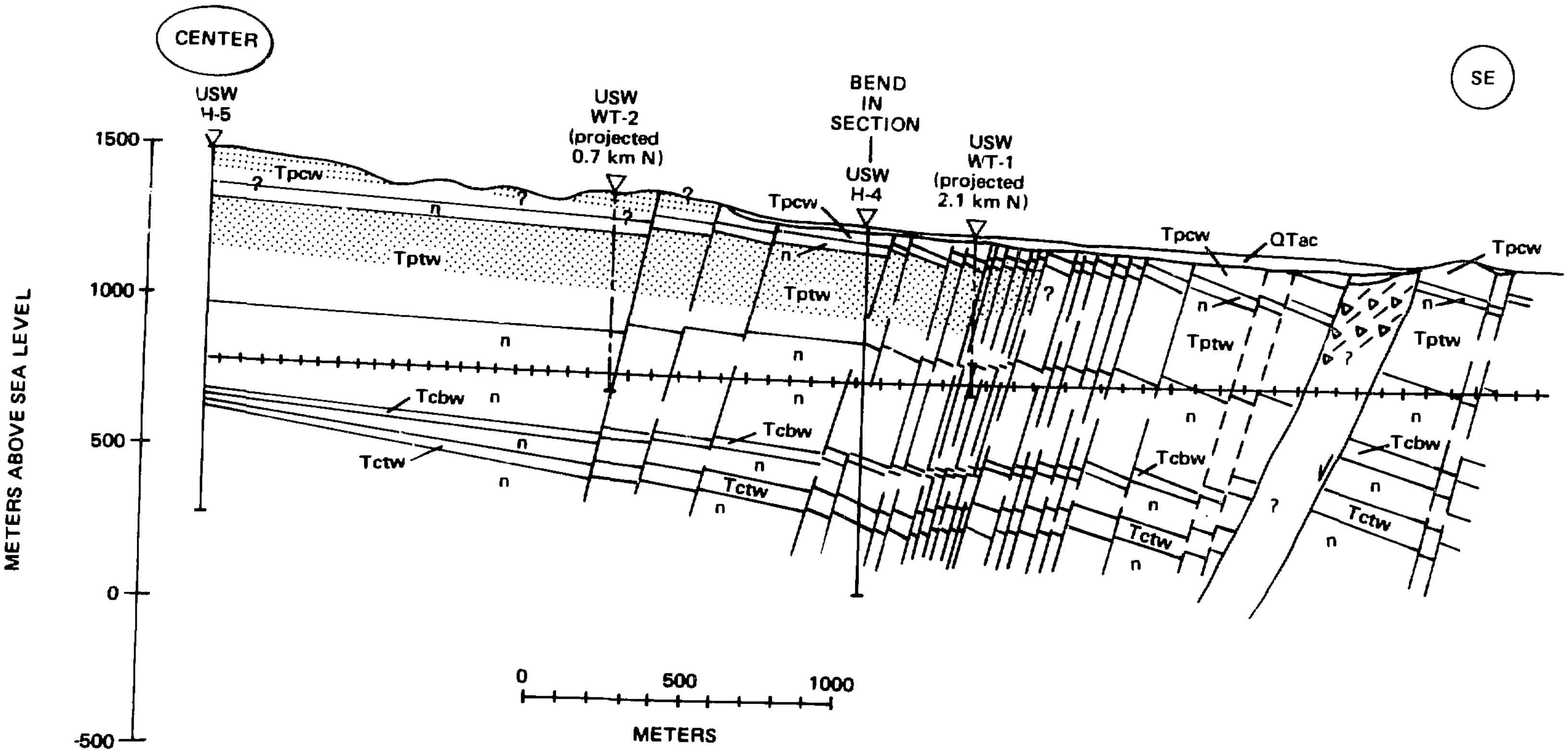

Tridymite

Fig. B-3 (cont)

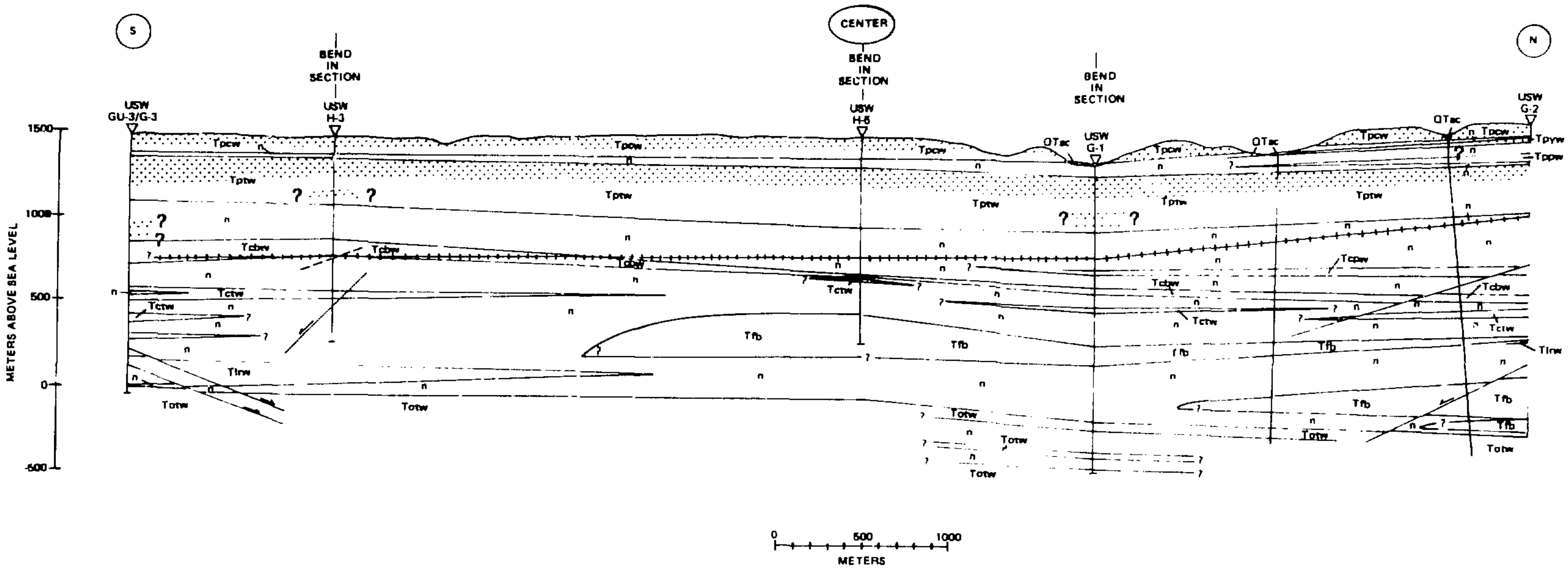

Tridymite

Fig. B-3 (cont)

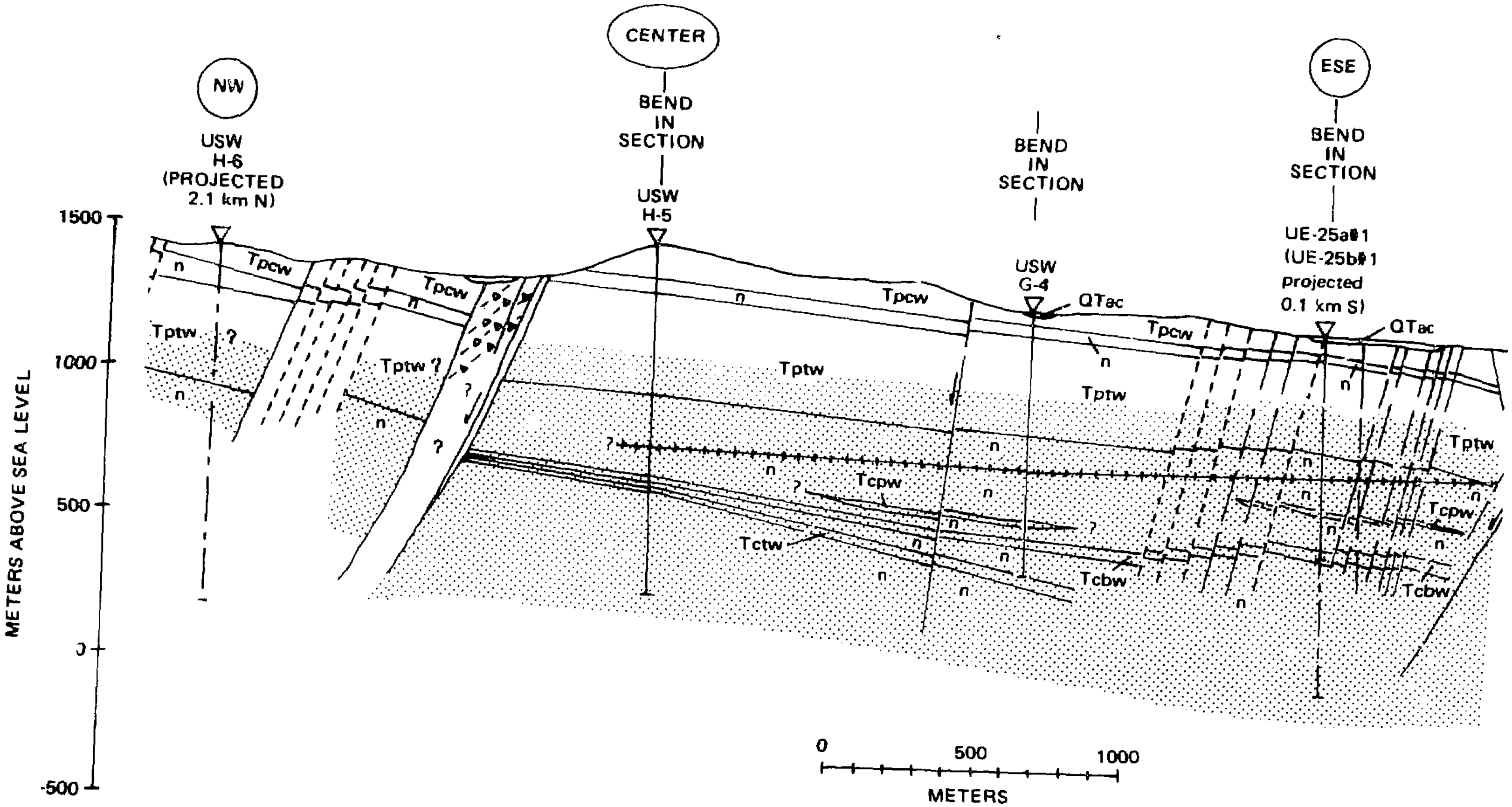

Quartz (zone of common and abundant occurrance)

Fig. B-4.
Distribution of quartz occurrences. Quartz may also occur above the level shown, but only as an isolated minor mineral or in veins. Symbols are defined in Fig. B-2.

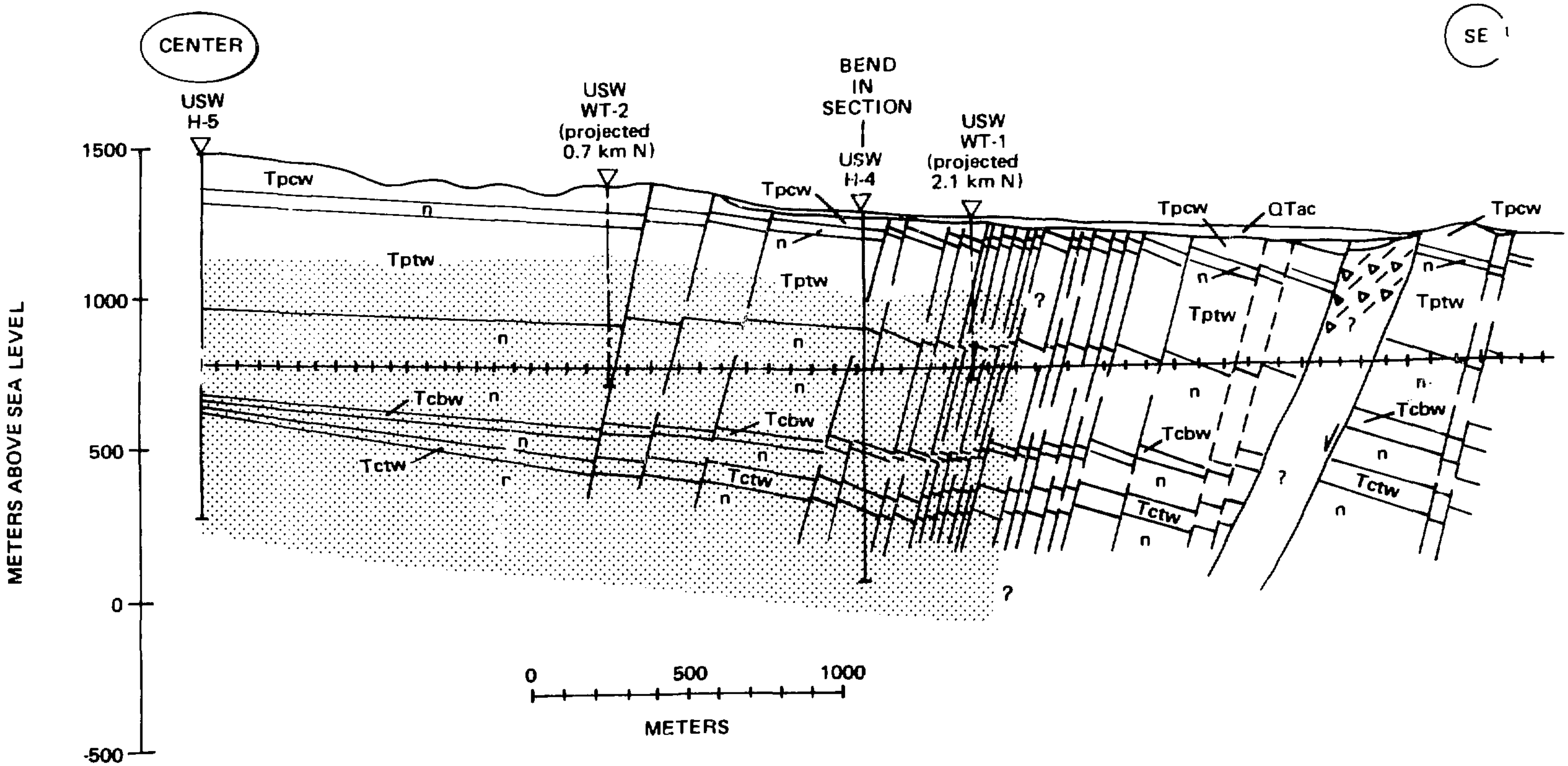

Quartz (zone of common and abundant occurrance)

Fig. B-4 (cont)

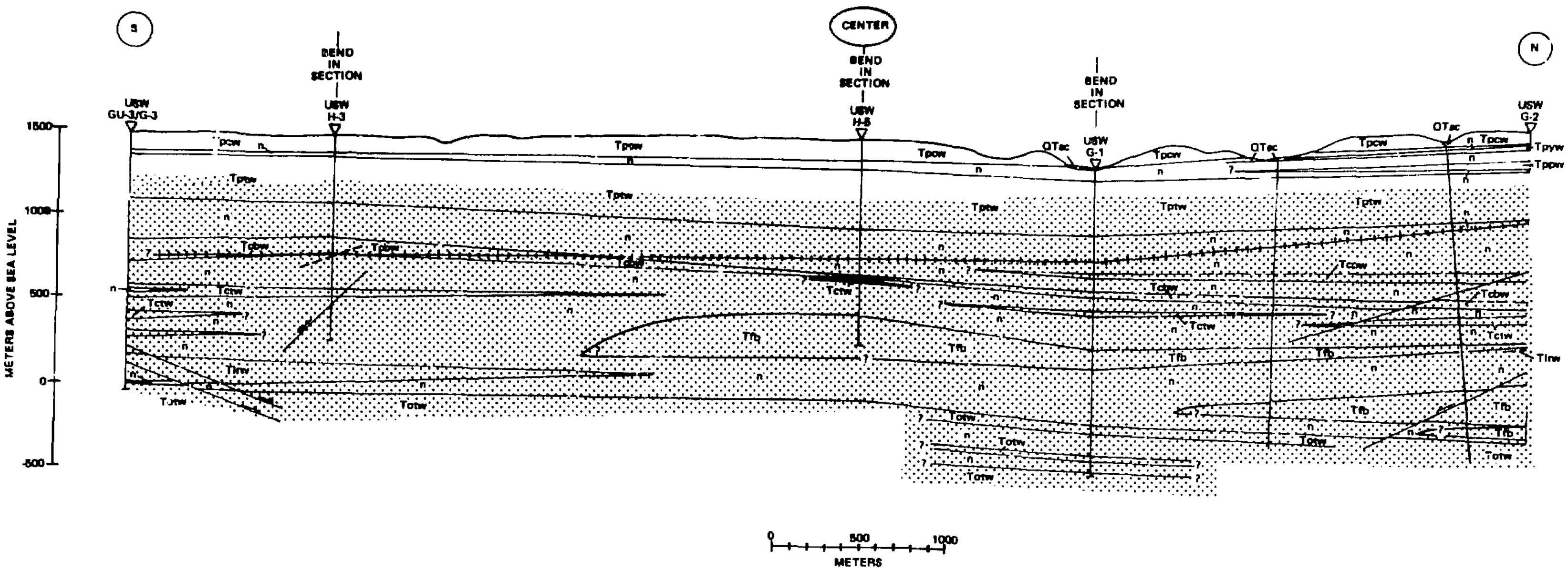

Quartz (zone of common and abundant occurrance)

Fig. B-4 (cont)

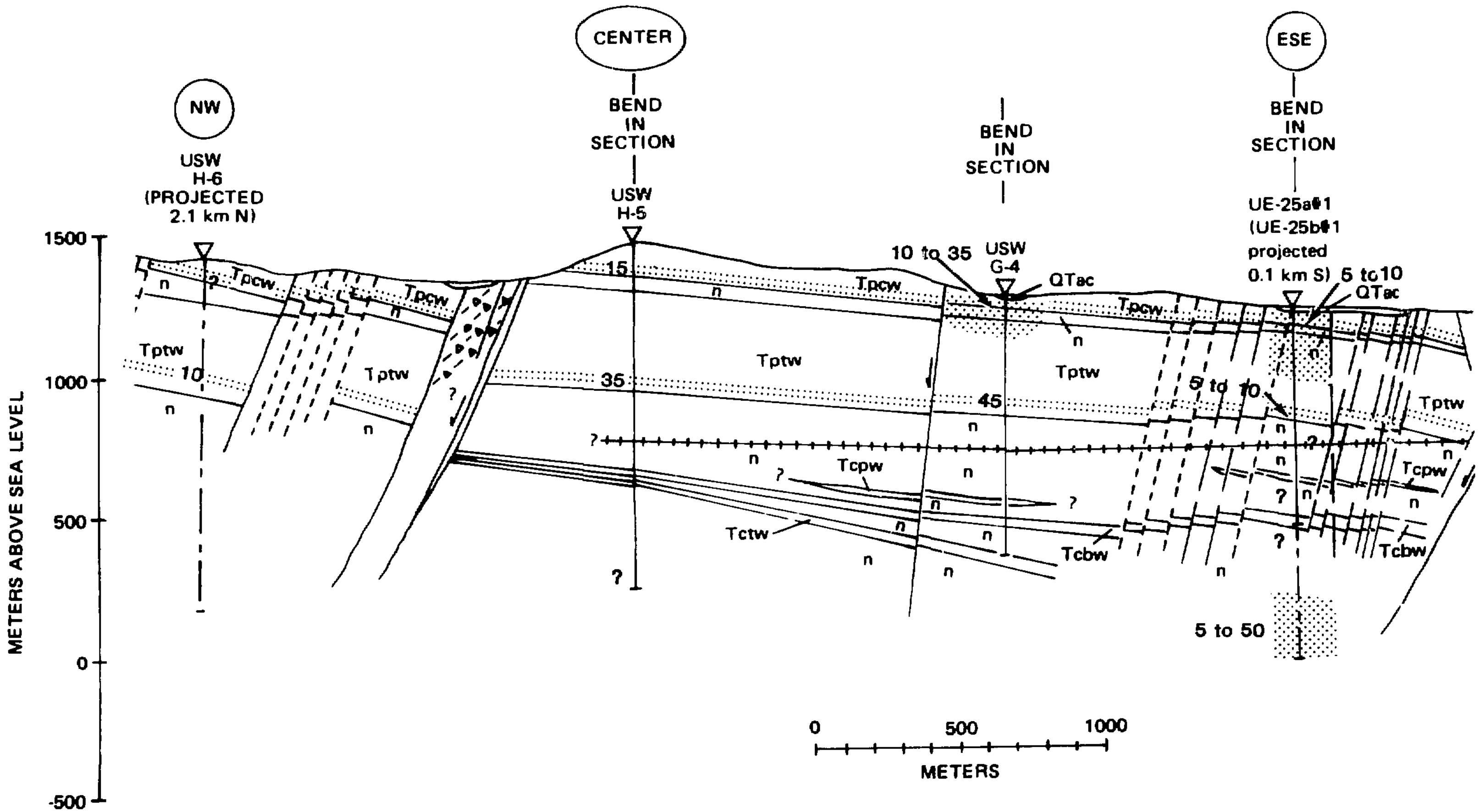

Smectite (>5%)

Fig. B-5.
Distribution of smectite, shown as percentage ranges of abundanc . Deeper occurrences may include appreciable interstratified illite. Symbols are defined in Fig. B-2.

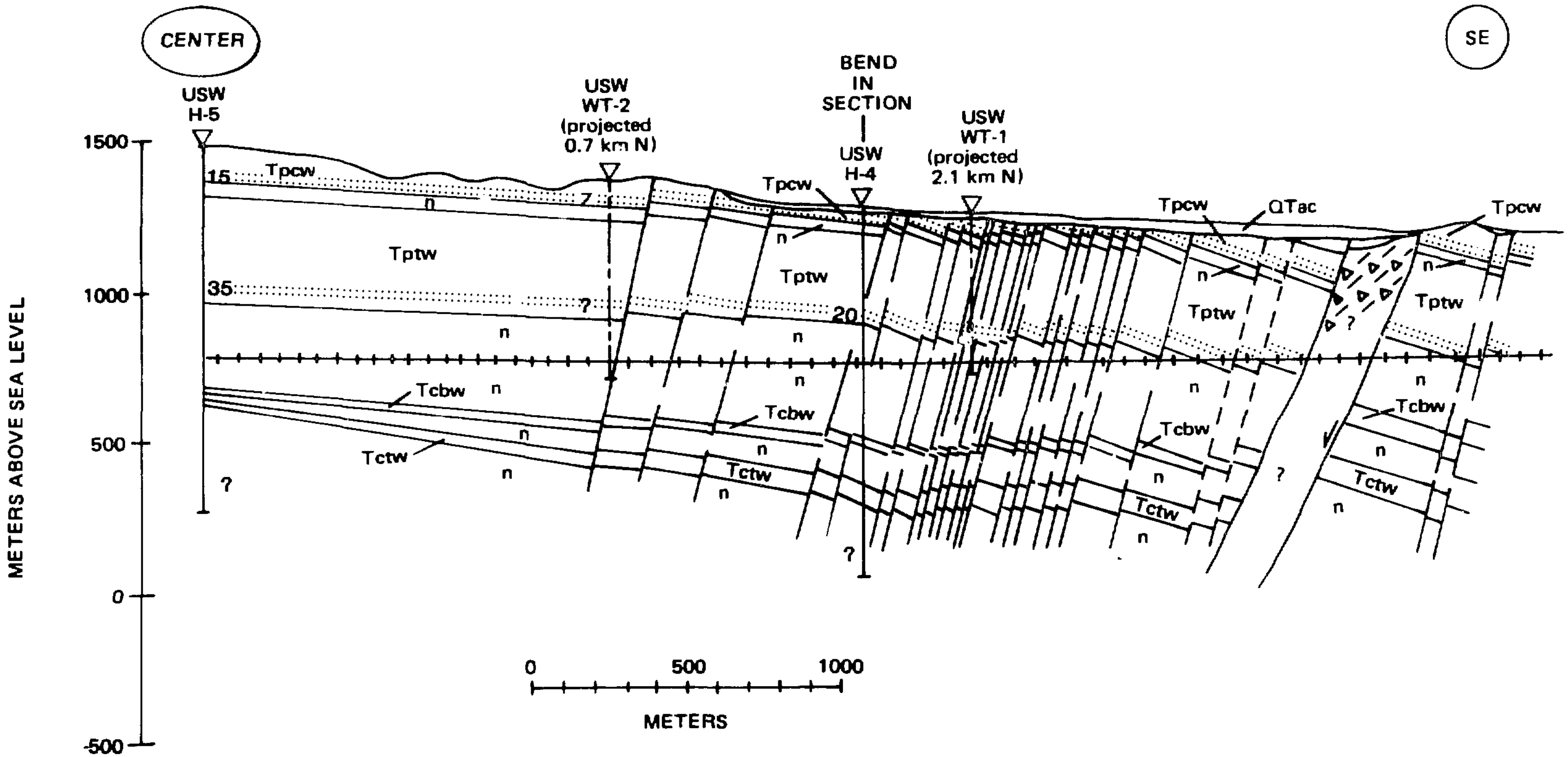

Smectite (>5%)

Fig. B-5 (cont)

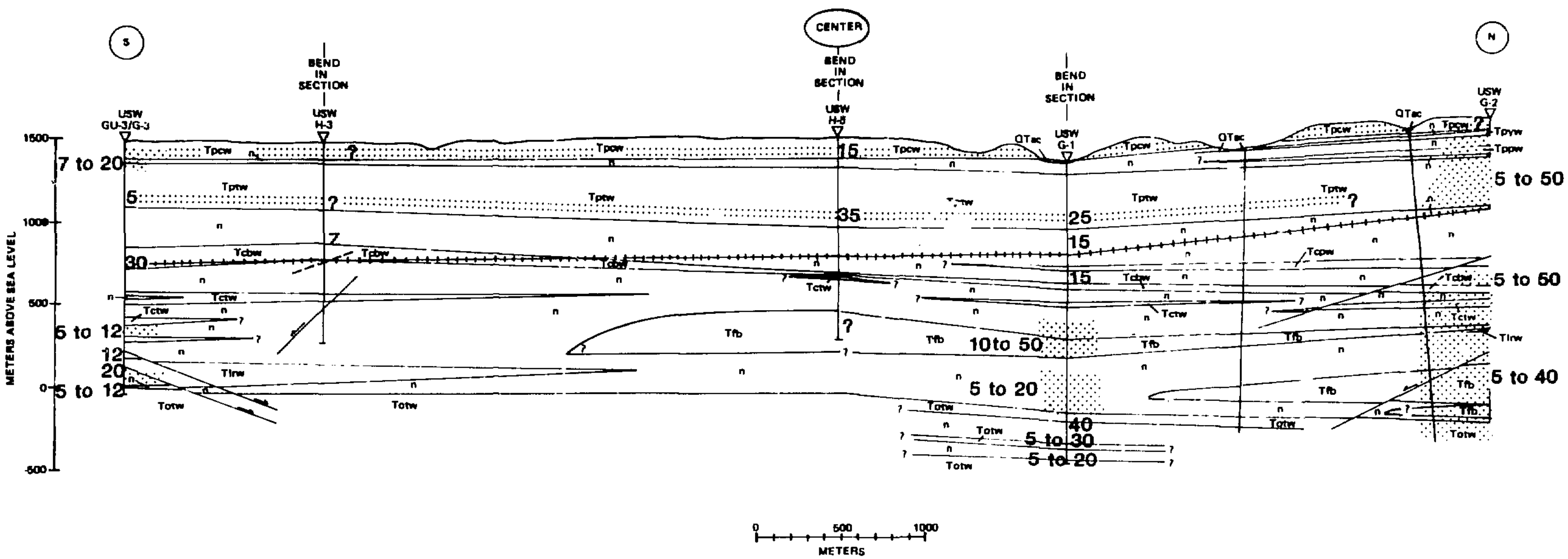

Smectite (>5%)

Fig. B-5 (cont)

APPENDIX B (cont)

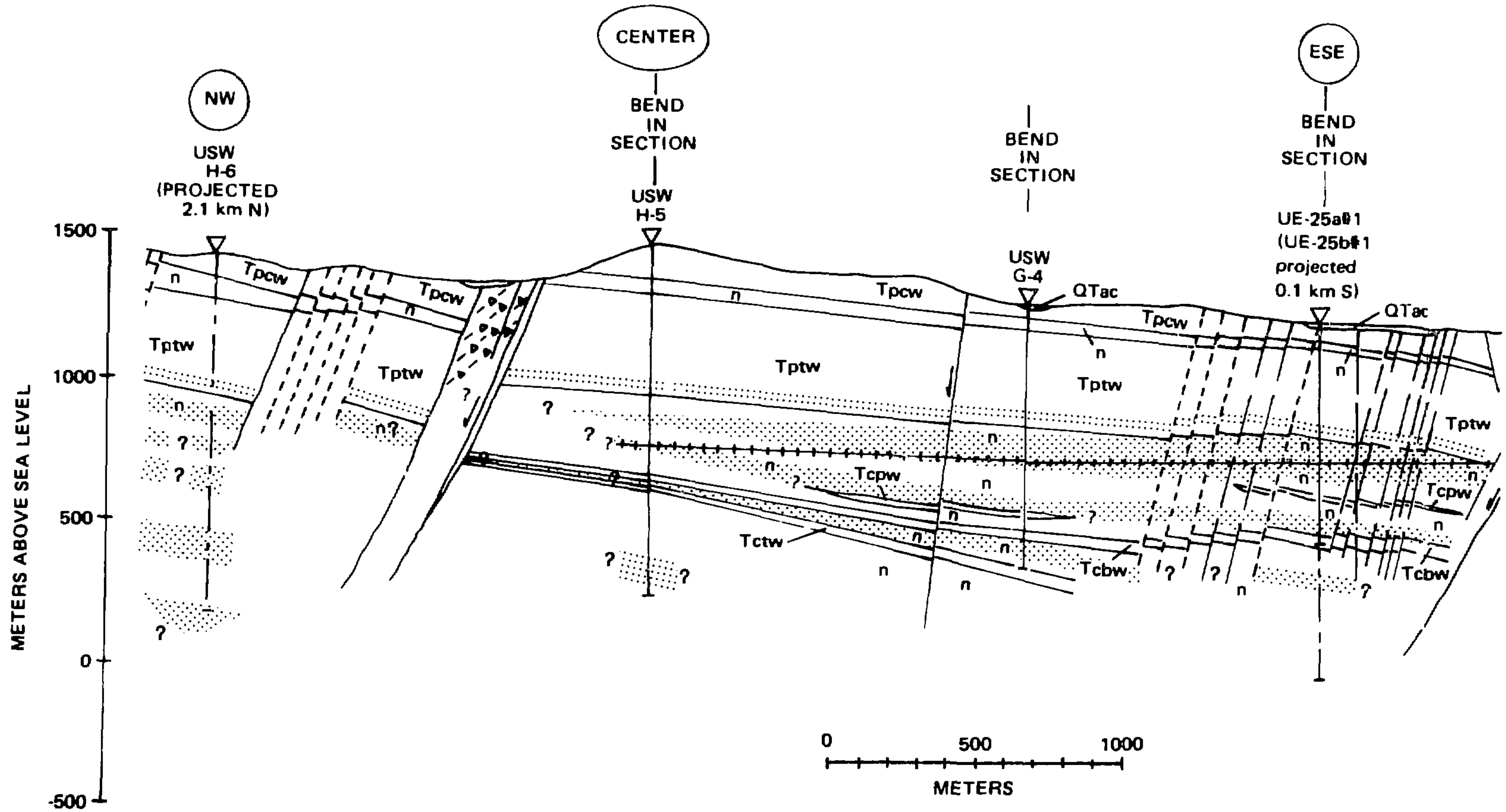

Major Clinoptilolite / Mordenite Intervals

H-5 below 760 m from Bentley, et al. (1983)
central part of H-6 from Craig, et al. (1983)

Fig. B-6.

Major intervals containing the sorptive minerals clinoptilolite or mordenite. The interval within the lower Tptw (above the basal vitrophyre--see Fig. B-2) consists mostly of heulandite (isostructural with clinoptilolite). Mordenite may be completely absent in some parts of some of these mapped intervals (e.g., in USW G-3 and GU-3). Symbols are defined in Fig. B-2.

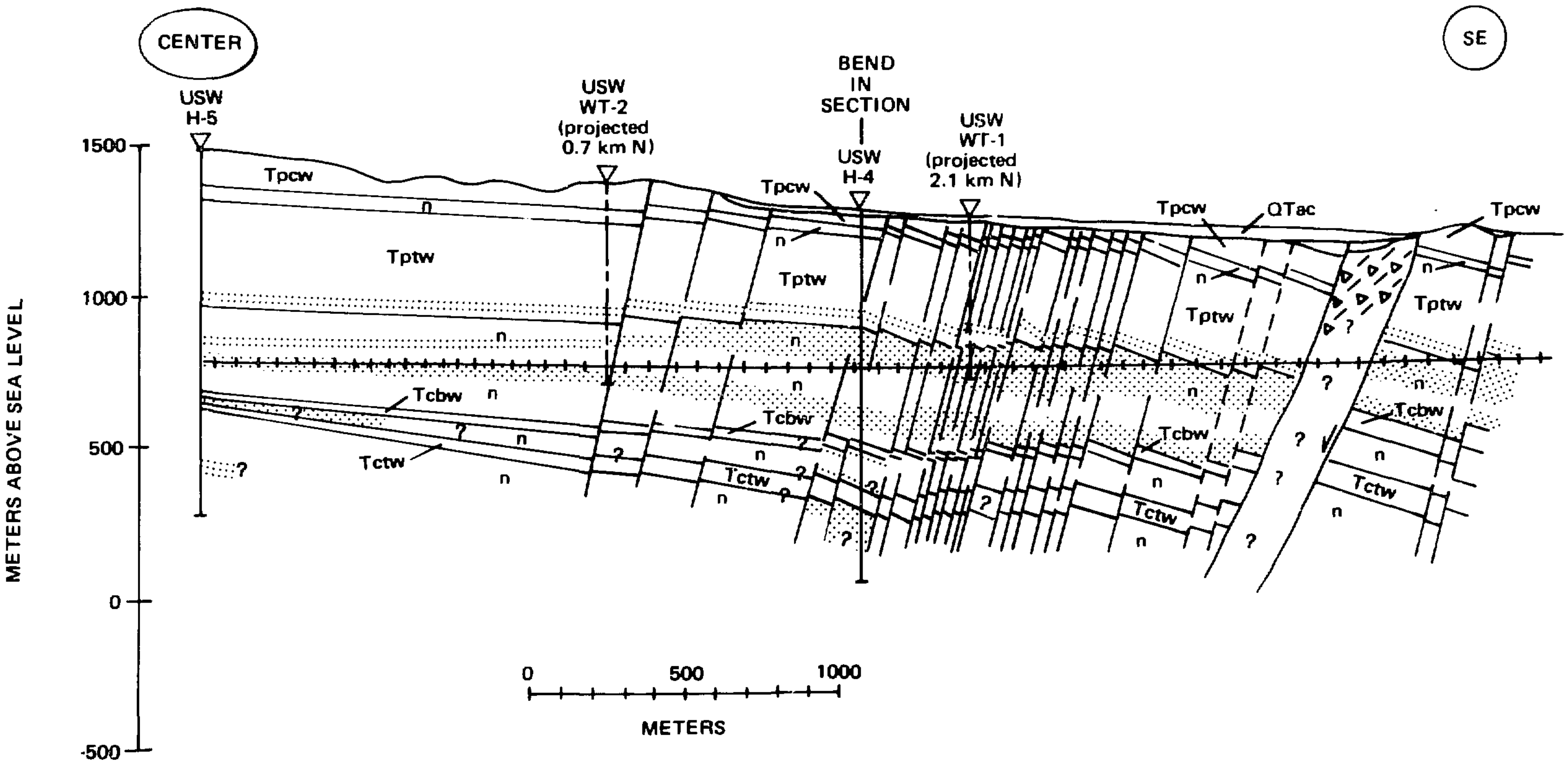

Major Clinoptilolite / Mordenite Intervals

Fig. B-6 (cont)

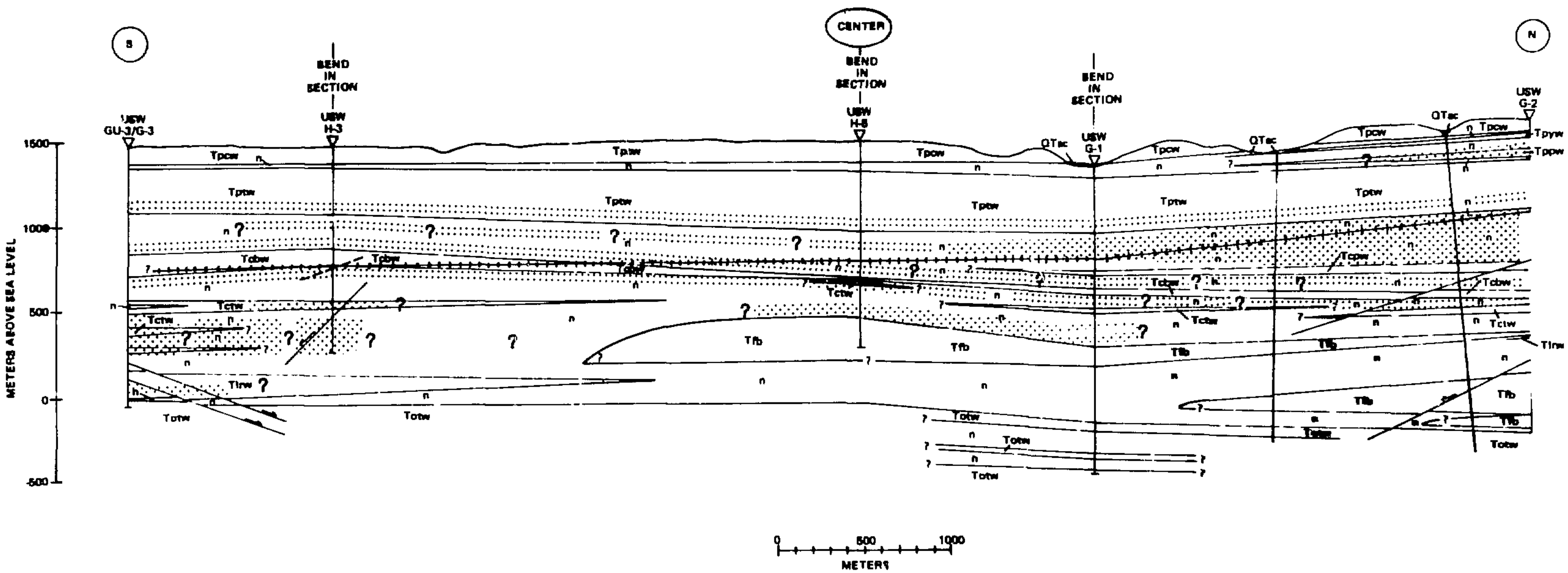

Major Clinoptilolite / Mordenite Intervals

Fig. B-6 (cont)

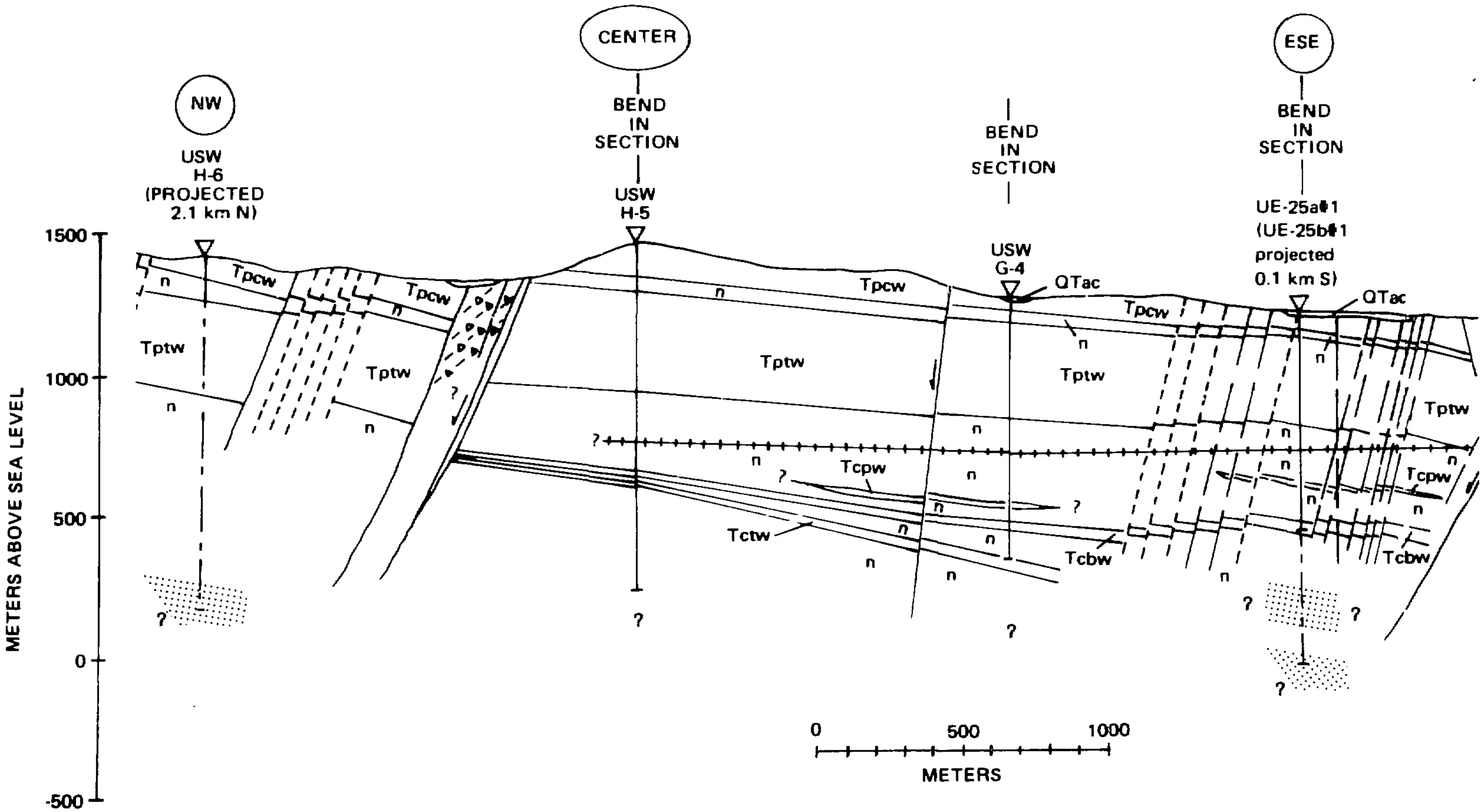

Analcime

Fig. B-7.
Distribution of analcime. Symbols are defined in Fig. B-2.

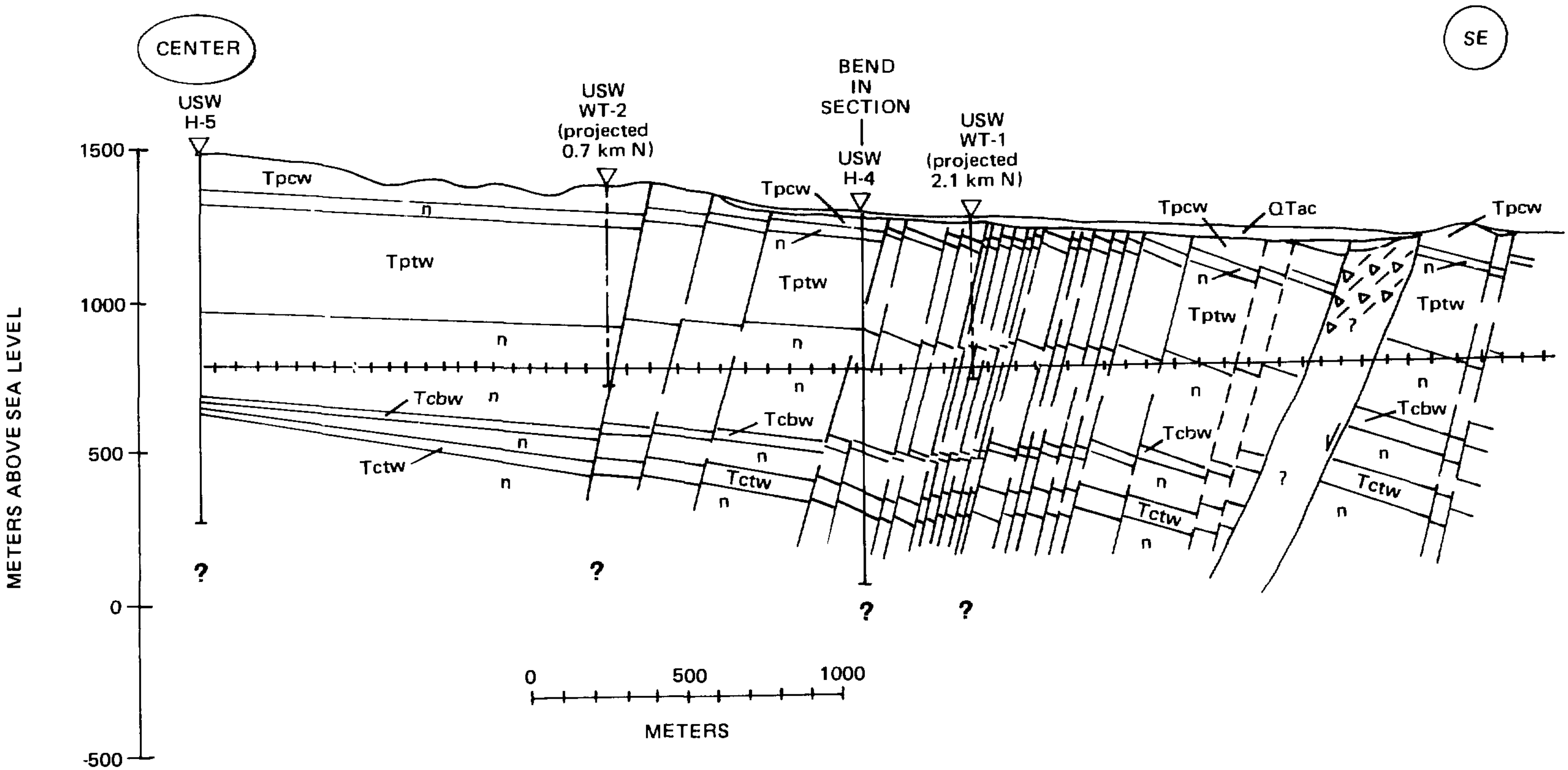

Analcime

Fig. B-7 (cont)

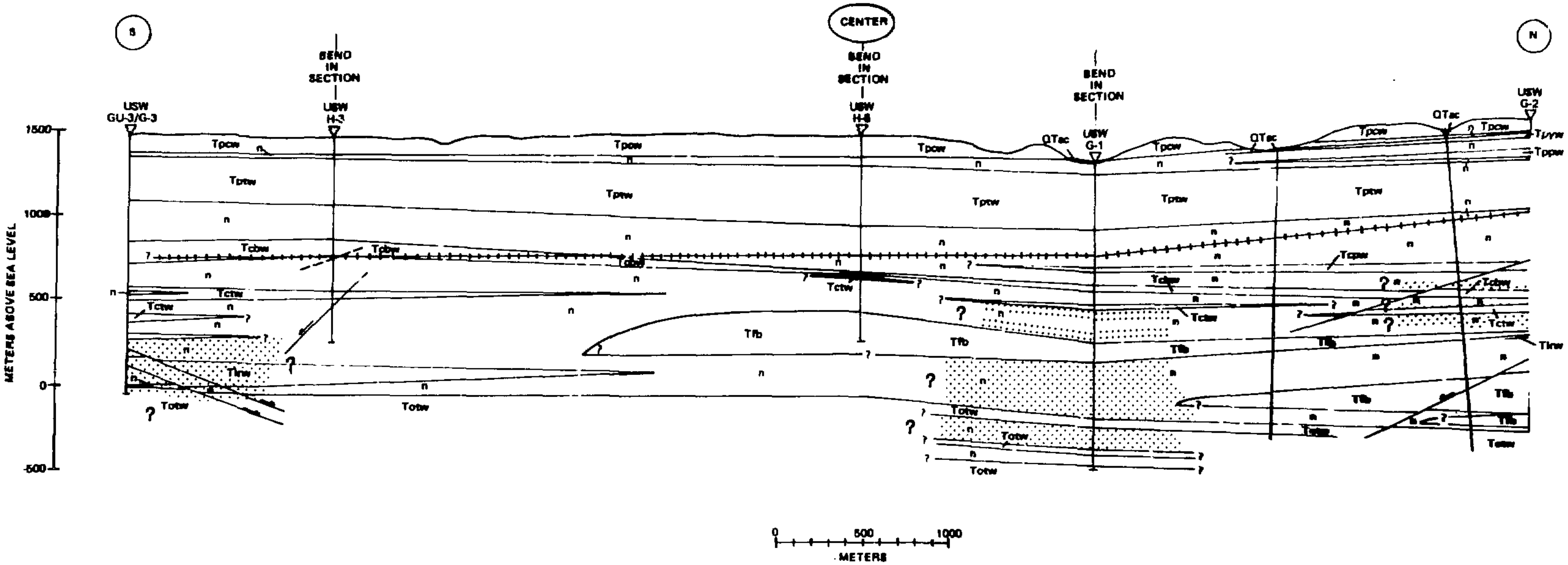

Analcime

Fig. B-7 (cont)

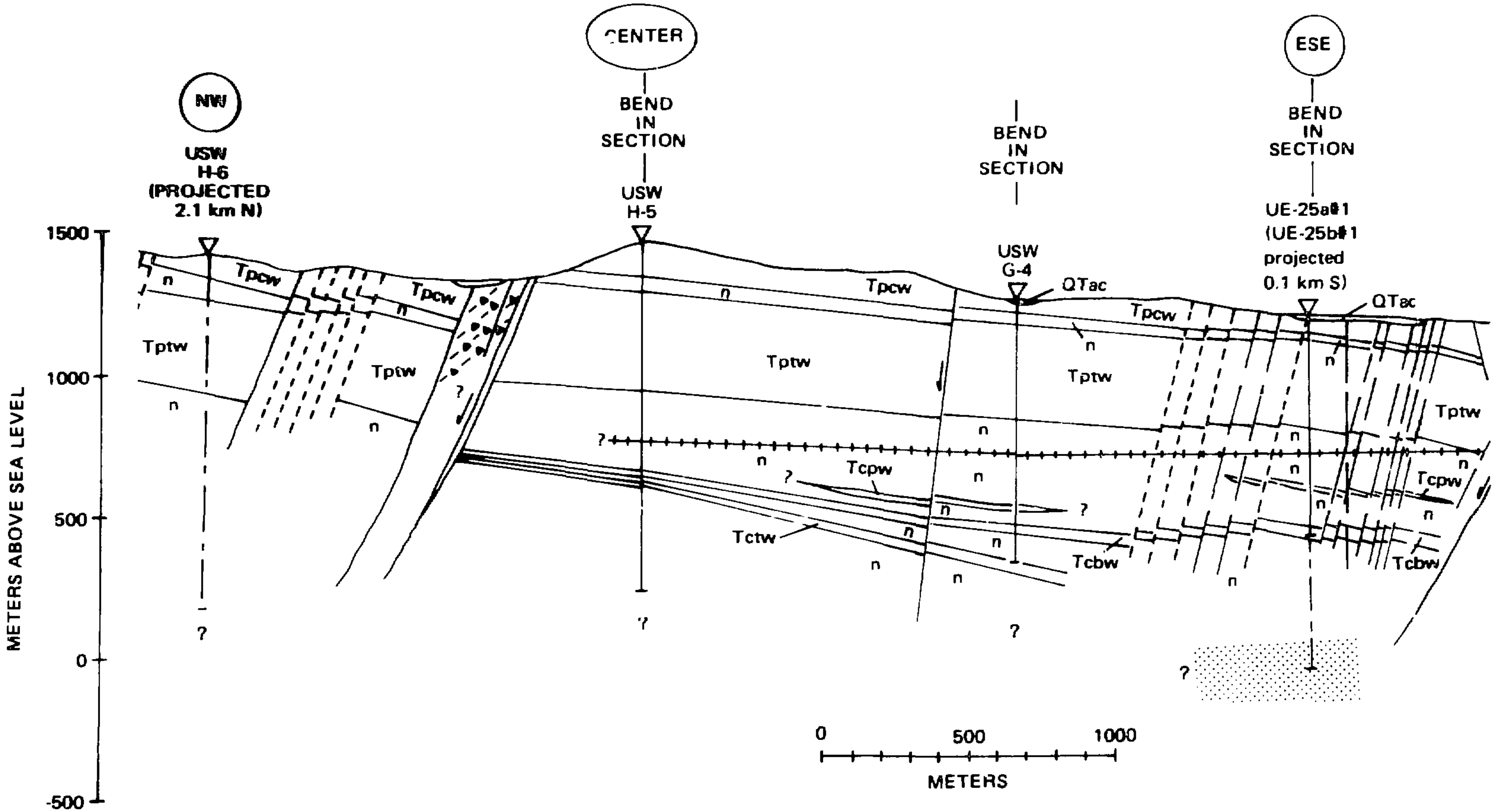

Authigenic Albite

Fig. B-8.

Distribution of authigenic albite (approximately pure albite with only minor potassium feldspar component). This distribution is determined by optical and electron microprobe studies (Bish et al. 1982; Caporuscio et al. 1982) rather than by x-ray diffraction. Symbols are defined in Fig. B-2.

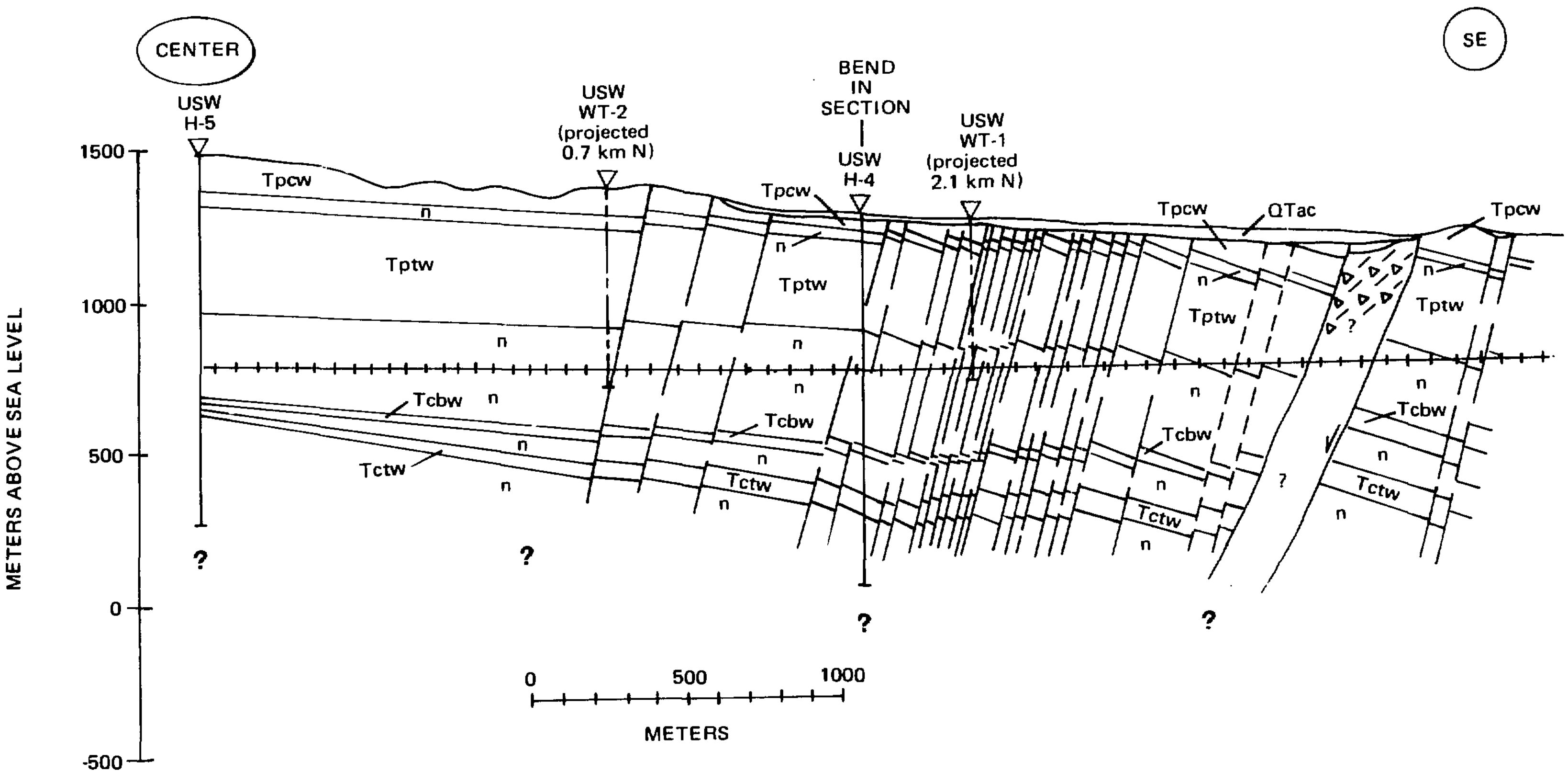

Authigenic Albite

Fig. B-8 (cont)

APPENDIX B (cont)

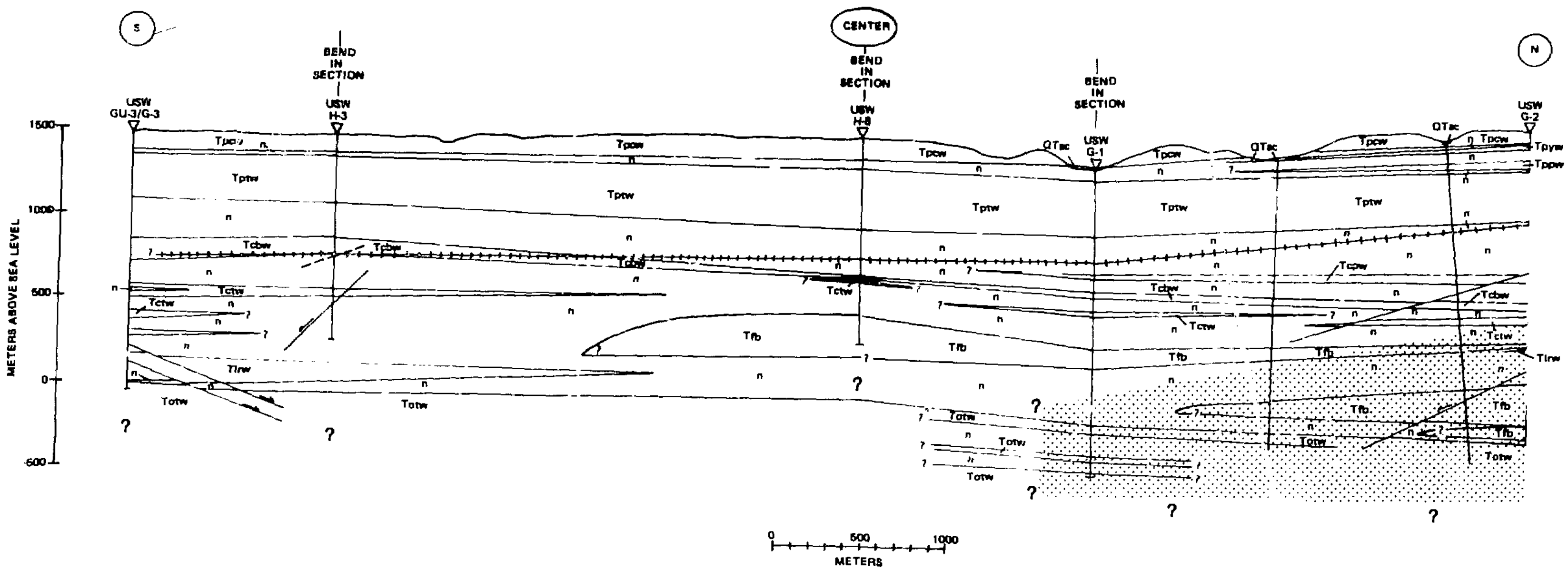

Authigenic Albite

Fig. B-8 (cont)

REFERENCES

Barth, T. F. W., Theoretical Petrology, John Wiley & Sons, Inc., New York (1952).

Bentley, C. B., J. H. Robison, and R. W. Spengler, "Geohydrologic Data for Test Well USW H-5 Yucca Mountain Area, Nye County, Nevada," U.S. Geological Survey Open File report 83-853 (1983).

Bish, D. L., F. A. Caporuscio, J. F. Copp, B. M. Crowe, J. D. Purson, J. R. Smyth, and R. G. Warren, "Preliminary Stratigraphic and Petrologic Characterization of Core Samples from USW-G1, Yucca Mountain, Nevada," Los Alamos National Laboratory report LA-8840-MS (November 1981).

Bish, D. L. and E. Semarge, "Mineralogic Variations in a Silicic Tuff Sequence: Evidence for Diagenetic and Hydrothermal Reactions," 19th Annual Clay Minerals Society Meeting, Hilo, Hawaii, August 8-14, 1982 (Abstract).

Bish, D. L., D. T. Vaniman, F. M. Byers, Jr., and D. E. Broxton, "Summary of the Mineralogy-Petrology of Tuffs of Yucca Mountain and the Secondary-Phase Thermal Stability in Tuffs," Los Alamos National Laboratory report LA-9321-MS (November 1982).

Bish, D. L., A. E. Ogard, D. T. Vaniman, and L. Benson, "Mineralogy-Petrology and Groundwater Geochemistry of Yucca Mountain Tuffs," in Scientific Basis for Nuclear Waste Management VII, Materials Research Society Symposia Proceedings, Boston (G. L. McVay, Ed.), 283-391 (1984a).

Bish, D. L., D. T. Vaniman, R. S. Rundberg, K. Wolfsberg, W. R. Daniels, and D. E. Broxton, "Natural Sorptive Barriers in Yucca Mountain, Nevada, for Long-Term Isolation of High-Level Waste," Radioactive Waste Management, Vol. 3, 415-432 (1984b).

Borg, I. Y. and D. K. Smith, Calculated X-ray Powder Patterns for Silicate Minerals, Geological Society of America, Memoir 122, 896 pp. (1969).

Byers, F. M., "Petrochemical Variation of Topopah Spring Tuff Matrix with Depth (Stratigraphic Level), Drill Hole USW G-4, Yucca Mountain, Nevada," Los Alamos National Laboratory report LA-10561-MS (December 1985).

Caporuscio, F., D. Vaniman, D. Bish, D. Broxton, B. Arney, G. Heiken, F. Byers, R. Gooley, and E. Semarge, "Petrologic Studies of Drill Cores USW-G2 and UE25b-1H, Yucca Mountain, Nevada," Los Alamos National Laboratory report LA-9255-MS (July 1982).

Caporuscio, F. A. and D. T. Vaniman, "Iron and Manganese in Oxide Minerals and in Glasses: Preliminary Consideration of Eh Buffering Potential at Yucca Mountain, Nevada," Los Alamos National Laboratory report LA-10369-MS, (April 1985).

Carlos, B. A., "Minerals in Fractures of the Unsaturated Zone from Drill Core USW G-4, Yucca Mountain, Nye County, Nevada," Los Alamos National Laboratory report LA-10415-MS (April 1985).

Carroll, P. I., F. A. Caporuscio, and D. L. Bish, "Further Description of the Petrology of the Topopah Spring Member of the Paintbrush Tuff in Drill Holes UE25A-1 and USW-G1, and of the Lithic Rich Tuff in USW-G1, Yucca Mountain, Nevada," Los Alamos National Laboratory report LA-9000-MS (November 1981).

Chung, F. H., "Quantitative Interpretation of X-ray Diffraction Patterns of Mixtures. I. Matrix-Flushing Method for Quantitative Multicomponent Analysis," Journal of Applied Crystallography, 7, 519-525 (1974a).

Chung, F. H., "Quantitative Interpretation of X-ray Diffraction Patterns of Mixtures. II. Adiabatic Principle of X-ray Diffraction Analysis of Mixtures," Journal of Applied Crystallography, 7, 526-531 (1974b).

Craig, R. W., R. L. Reed, and R. W. Spengler, "Geohydrologic Data for Test Well USW H-6 Yucca Mountain Area, Nye County, Nevada," U.S. Geological Survey Open File report 83-856 (1983).

Gillery, F. H., "Adsorption-Desorption Characteristics of Synthetic Montmorillonoids in Humid Atmospheres," American Mineralogist, 44, 806-818 (1959).

Heiken, G. H. and M. L. Bevier, "Petrology of Tuff Units from the J-13 Drill Site, Jackass Flats, Nevada," Los Alamos National Laboratory report LA-7563-MS (February 1979).

Hoover, D. L., "Genesis of Zeolites, Nevada Test Site," in Nevada Test Site, Geological Society of America, Memoir 110, 275-284 (1968).

Jones, B. F., "Mineralogy of Fine Grained Alluvium from Borehole U11g, Expl. 1, Northern Frenchman Flat Area, Nevada Test Site," U.S. Geological Survey Open-File report 82-765 (1982).

Klug, H. P. and L. E. Alexander, X-ray Diffraction Procedures for Polycrystalline and Amorphous Materials, John Wiley & Sons, Inc., New York (1974).

Knauss, K. G., V. M. Oversby, and T. J. Wolery, "Post Emplacement Environment of Waste Packages," in Scientific Basis for Nuclear Waste Management VII, Materials Research Society Symposia Proceedings, Boston (G. L. McVay, Ed.), 301-308 (1984).

Lappin, A. R., "Bulk and Thermal Properties of the Functional Tuffaceous Beds in Holes USW-G1, UE25A#1, and USW-G2, Yucca Mountain, Nevada," Sandia National Laboratories report SAND82-1434 (1982).

Lappin, A. R., R. G. VanBuskirk, D. O. Enniss, S. W. Butters, F. M. Prater, C. B. Muller, and J. L. Bergosh, "Thermal Conductivity, Bulk Properties, and Thermal Stratigraphy of Silicic Tuffs from the Upper Portion of Hole USW-G1, Yucca Mountain, Nye County, Nevada," Sandia National Laboratories report SAND81-1873 (March 1982).

Levy, S. S., "Petrology of Samples from Drill Holes USW H-3, H-4, and H-5, Yucca Mountain, Nevada," Los Alamos National Laboratory report LA-9706-MS (June 1984a).

Levy, S. S., "Studies of Altered Vitrophyre for the Prediction of Nuclear Waste Repository-Induced Thermal Alteration at Yucca Mountain, Nevada," in Scientific Basis for Nuclear Waste Management VII, Materials Research Society Symposia Proceedings, Boston (G. L. McVay, Ed.), 959-966 (1984b).

Moncure, G. K., R. C. Surdam, and H. L. McKague, "Zeolite Diagenesis Below Pahute Mesa, Nevada Test Site," Clays and Clay Minerals, 29, 385-396 (1981).

Price, R. H., S. J. Spence, and A. K. Jones, "Uniaxial Compression Test Series on Topopah Spring Tuff from USW GU-3, Yucca Mountain, Southern Nevada," Sandia National Laboratories report SAND83-1646 (February 1984).

Scott, R. and J. Bonk, "Geological Map of Yucca Mountain with Cross Sections," U.S. Geological Survey Open File report 84-494 (1984).

Smyth, J. R., "Zeolite Stability Constraints on Radioactive Waste Isolation in Zeolite-Bearing Volcanic Rocks," Journal of Geology 90, 195-201 (1982).

Suquet, H., C. De La Calle, and H. Pezerat, "Swelling and Structural Organization of Saponite," Clays and Clay Minerals, 23, 1-9 (1975).

Sykes, M. L., G. H. Heiken, and J. R. Smyth, "Mineralogy and Petrology of Tuff Units from the UE25a-1 Drill Site, Yucca Mountain, Nevada," Los Alamos National Laboratory report LA-8139-MS (November 1979).

Vaniman, D., D. Bish, D. Broxton, F. Byers, G. Heiken, B. Carlos, E. Semarge, F. Caporuscio, and R. Gooley, "Variations in Authigenic Mineralogy and Sorptive Zeolite Abundance at Yucca Mountain, Nevada, Based on Studies of Drill Cores USW GU-3 and G-3," Los Alamos National Laboratory report LA-9707-MS (June 1984).

Zielinsky, R. A., "Evaluation of Ash-Flow Tuffs as Hosts for Radioactive Waste: Criteria Based on Selective Leaching of Manganese Oxides," U.S. Geological Survey Open-File report 83-480 (1983).